

**MODELING AND THERAPEUTIC TARGETING OF  
ENDOGENOUS *IDH1*-MUTANT GLIOMA**

by  
Alexandra Borodovsky

A dissertation submitted to Johns Hopkins University in conformity with the  
requirements for the degree of Doctor of Philosophy

Baltimore, Maryland  
March, 2014

© 2014 Alexandra Borodovsky  
All Rights Reserved

## **ABSTRACT**

Somatic mutations in *Isocitrate Dehydrogenase 1 (IDH1)* are frequent in low grade and progressive gliomas. *IDH1* mutant tumors are phenotypically characterized by the increased production of 2-hydroxyglutarate (2-HG) from  $\alpha$ -ketoglutarate. 2-HG is an “oncometabolite” that competitively inhibits  $\alpha$ -KG dependent dioxygenases. The inhibition of these dioxygenases causes widespread cellular changes including abnormal hypermethylation of genomic DNA and suppression of cellular differentiation. Recent investigations of malignant gliomas have identified additional genetic and chromosomal abnormalities that cluster with *IDH1* mutations into two molecularly distinct subgroups. The astrocytic subgroup is defined by frequent mutations in *ATRX*, *TP53* and displays alternative lengthening of telomeres. The second subgroup with oligodendrocytic morphology has frequent mutations in *CIC* or *FUBP1*, and is linked to co-deletion of the 1p/19q arms. These mutations reflect the development of two distinct molecular pathways representing the majority of *IDH1* mutant gliomas. Unfortunately, due to the scarcity of endogenously derived *IDH1* mutant models, opportunities to evaluate therapies targeted to the mutation or its consequences have been limited.

Here we report the generation of an endogenous *IDH1* mutant anaplastic astrocytoma model. This novel tumor model expresses the IDH1 (R132H) mutant protein, grows rapidly *in vivo*, produces 2-HG, exhibits DNA hypermethylation and harbors concurrent mutations in *TP53*, *CDKN2A* and *ATRX*. Furthermore, this model has a similar histopathology as the original patient tumor, and exhibits an alternative lengthening of telomeres phenotype.

Using this *in vivo* model, we have demonstrated the preclinical efficacy and mechanism of action of the FDA approved demethylating drug 5-azacytidine. Long term administration of 5-azacytidine resulted in reduction of DNA methylation of promoter loci, induction of glial differentiation, reduction of cell proliferation and a significant reduction in tumor growth. Tumors regressed by 14 weeks and subsequently showed no signs of re-growth at 7 weeks despite discontinuation of therapy. These results suggest that demethylating agents might be useful for the clinical management of patients with IDH-mutant gliomas.

Advisor: Dr. Gregory J. Riggins

Reader: Dr. Fred Bunz

Committee: Dr. Gregory J. Riggins

Dr. Fred Bunz

Dr. Robert A. Casero Jr.

Dr. Takashi Tsukamoto

## ACKNOWLEDGEMENTS

First and foremost, I would like to thank my thesis advisor Dr. Gregory Riggins for his outstanding guidance and mentorship. When I first emailed Greg with regards to rotating in his lab, he informed me that although he could not take a student due to funding, he would be happy to meet with me just to chat about brain cancer. Thanks to the delusional optimism that comes with being a first year graduate student, I figured that things would somehow work out. Astoundingly, my presumption was confirmed the following week when Greg informed me that his grant had just been funded and that I was welcome to join the lab. From then on, Greg has trained me how to be a better scientist through his profound knowledge and insight. Additionally, Greg has exhibited outstanding patience and dedication by consistently regarding my scientific ideas with earnestness and enthusiasm, even going so far as to wager a bucket of steamed crabs on a scientific outcome.

I am very grateful for the contributions of my lab members, both past and present, for technical assistance, constructive support and for creating a collaborative atmosphere. Thank you Avadhut Joshi, Vafi Salmasi, Gilson Baia, I-Mei Siu, Qi Zhao, Tara Williamson, Nee Sawanyawisuth, Zev Binder, Colette ap Rhys, Reny Bai, Verena Staedtke, Genevieve Weber, Otavia Caballero, Gary Gallia, Callen Riggins, and Brenda Raymond.

I owe a large debt of gratitude to Meghan Seltzer for laying the foundation of my graduate research and for teaching me the skills with which to study this fascinating project. I also thank Kelli Wilson for meticulously overseeing each and every animal study when I was unable to make it into lab, and for her friendship through these last four

years. Kelli not only aided in the success of my project (it was she who suggested I email Greg about a lab rotation), but also made it enjoyable to come to lab every day.

I would like to thank those who served on my thesis committee: Fred Bunz, Robert Casero, and Takashi Tsukamoto. In addition to their valuable feedback during our meetings, I have had the pleasure of working with each of these outstanding scientists on independent projects, which has aided in my training immensely. Thank you also to the contributions of Alan Meeker, Charles Eberhart, Tim Chan, Michael Collector, James Eshelman, Steve Baylin, and Bert Vogelstein in my thesis project.

I am grateful to the Cellular and Molecular Medicine Graduate Program for not only accepting me into the program but for then making the experience so spectacularly fulfilling. Thank you to Colleen Graham, Leslie Lichter, Rajni Rao and Robert Casero. Thank you also to my fellow CMM classmates for being a constant source of merriment, support and commiseration.

In the completion of this work, there are several core facilities without which my project would have been significantly more challenging. Thanks to Michelle Rudek at the LC/MS core, Roxann Ashworth and Laura Kasch at the Genomics Core Resource Facility, Wayne Yu at the Tissue Microarray Core, Rudy Der at the Immunopathology core, the team in the Histopathology core. A special thanks to the members of the CRB2 animal facility for their constant vigilance regarding the wellbeing of my mice.

I am exceedingly grateful to my family who has been essential to my success. I know it wasn't easy for me to be so far from Oregon, and I cannot thank you enough for your unconditional love and support during this time. Thank you to my father for his incredible love, guidance and for always believing in me. I owe him a particular debt of

gratitude for encouraging me to peruse laboratory job out of college rather than one in a department store, as was my inclination at the time. Thank you to my mother who has always been a pillar of strength and love in my life. Her insightful advice and encouragement has allowed me to grow emotionally and intellectually. Thank you both for pushing me to reach my potential and for teaching me to not sweat the small stuff.

Finally, I would like to thank my best friend and partner, Andrew Larsen. Since the beginning of my time at Hopkins, Andrew has been my closest companion, my greatest supporter and a powerful motivator. He has provided constant academic support and I am eternally grateful for his encouragement in revisiting the 5-azacytidine project for *IDH1* mutant glioma. His non-academic contributions are too vast to recount suffice it to say that without his extraordinary friendship, encouragement and support I would not have achieved my goal of earning a doctorate.

# TABLE OF CONTENTS

<b>ABSTRACT</b> .....	2
<b>ACKNOWLEDGEMENTS</b> .....	4
<b>LIST OF TABLES</b> .....	8
<b>LIST OF FIGURES</b> .....	8
<b>CHAPTER ONE: Metabolic and epigenetic alteration in <i>IDH1/2</i> mutant glioma</b> .....	10
<b>CHAPTER TWO: Development and characterization of a novel model of a patient-derived <i>IDH1</i> mutant glioma with alternative lengthening of telomeres</b> .....	25
INTRODUCTION .....	25
MATERIALS AND METHODS.....	27
RESULTS AND DISCUSSION .....	33
CONCLUSIONS .....	46
<b>CHAPTER THREE: 5-Azacytidine reduces methylation, promotes differentiation and induces tumor regression in a patient-derived <i>IDH1</i> mutant glioma xenograft</b> .....	47
INTRODUCTION .....	47
MATERIALS AND METHODS.....	49
RESULTS .....	52
DISCUSSION .....	62
<b>CHAPTER FOUR: Future directions of 5-azacytidine therapy for <i>IDH1</i> mutant gliomas</b> .....	65
<b>REFERENCES</b> .....	80
<b>CURRICULUM VITAE</b> .....	89

## LIST OF TABLES

### **Chapter One**

Table 1.1 Pathways potentially altered by IDH1/2 mutations in glioma.....	19
---	----

### **Chapter Two**

Table 2.1 Genetic Mutations in JHH-273.....	43
---	----

## LIST OF FIGURES

### **Chapter One**

Figure 1.1 Epigenetic and metabolic alterations in IDH1/2 mutant tumor cells. ....	13
Figure 1.2 Comparison of the structure of $\alpha$ -ketoglutarate and 2-hydroxyglutarate.....	16

### **Chapter Two**

Figure 2.1 Characteristic histological and genetic features of the IDH1 (R132H) anaplastic astrocytoma model.....	35
Figure 2.2 Infiltrative growth pattern of orthotopically implanted JHH-273.....	36
Figure 2.3 Growth of JHH-273 <i>in vivo</i> .....	38
Figure 2.4 2-HG production in JHH-273.....	40
Figure 2.5 ALT characterization in JHH-273.....	45

### **Chapter Three**

Figure 3.1 JHH-273 shows characteristic DNA hypermethylation which can be reversed with 5-azacytidine treatment <i>in vivo</i> . ....	54
---	----



Figure 3.2 Treatment strategy for 5-azacytidine in the IDH1 mutant flank model.....	56
Figure 3.3 Long term treatment with 5-azacytidine reduces tumor growth in an IDH1 mutant model .....	57
Figure 3.4 Treatment with 5-azacytidine induces differentiation in an <i>in vivo</i> IDH1 (R132H) glioma model.....	60
Figure 3.5 Treatment with 5-azacytidine induces differentiation and reduces the proliferative index in an <i>in vivo</i> IDH1 (R132H) glioma model.....	61

#### **Chapter Four**

Figure 4.1 Pretreatment of IDH1 mutant cells with 5-azacytidine extends survival in orthotopically implanted tumors.....	67
Figure 4.2 5-azacytidine pretreated tumors retain TMZ sensitivity <i>in vivo</i> .....	70
Figure 4.3 Targeting epigenetic reprogramming caused by oncometabolite 2-HG.....	74

## CHAPTER 1

### **METABOLIC AND EPIGENETIC ALTERATIONS IN *IDH1/2* MUTANT GLIOMAS**

Gliomas are a collection of nervous system tumors arising from glial cells such as astrocytes and oligodendroglia. The most deadly and aggressive of these gliomas is the grade IV astrocytomas, or glioblastoma multiforme (GBM). To better understand the genetic basis of GBM, 22 GBM genomes were sequenced. This study quantified the frequency of previously known mutations (e.g. *TP53*, *EGFRvIII*, *PI3KCA*) and led to the discovery of acquired mutations in *IDH1*, that were not previously known or associated with cancer [1]. Subsequent studies discovered mutations in *IDH2*, the mitochondrial homologue of *IDH1* [2]. There has been progress understanding the role of *IDH1/2* mutation in tumor formation and maintenance and recent findings have implicated altered enzymatic activity producing metabolic changes that ultimately disrupt normal epigenetics as likely contributing mechanisms.

#### *Metabolism and Cancer*

Associations between metabolism and cancer were first documented in the 1920's by Otto von Warburg. Warburg demonstrated that cancer cells exhibited increased rates of glycolysis and decreased dependence on oxidative phosphorylation, despite the presence of sufficient oxygen [3, 4]. Recently, the goals of understanding and therapeutically exploiting altered metabolism in cancer cells have received renewed interest. Oncogenes and tumor suppressors (e.g. *MYC*, *TP53*, *PI3KCA*, etc.) contribute to the altered regulation of metabolism in tumors, and the unmutated versions of these genes

play roles in normal cell metabolism [5-7]. However, relatively few mutations in genes encoding metabolic enzymes are known to contribute to oncogenesis. Known mutations include succinate dehydrogenase (*SDH*), fumarate dehydrogenase (*FH*), and *IDH1/2* [1, 6-8]. *SDH* and *FH* mutations are associated with familial cancer syndromes and lead to enzymatic inactivation, with subsequent accumulation of their respective substrates, succinate and fumarate. Accumulation of these metabolites contributes to tumorigenesis by stabilizing HIF-1 $\alpha$  in the presence of normoxic conditions through inhibition of prolyl hydroxylase domain 2 (PHD2). PHD2 utilizes O<sub>2</sub> and  $\alpha$ -ketoglutarate ( $\alpha$ -KG) to hydroxylate HIF-1 $\alpha$ , leading to its degradation. Inhibition of PHD2 in the presence of sufficient oxygen leads to increased HIF-1 $\alpha$  and promotes tumorigenesis through increased glycolysis and angiogenesis [6-10].

#### *IDH1/2 mutation frequency*

GBMs develop *de novo* (primary) or develop from lower grade gliomas (secondary). Mutations in *IDH1/2* occur in up to 70% of low grade gliomas and secondary GBMs [2] and in up to 12% of all primary GBMs [1]. *IDH1* and *IDH2* mutations also occur in 16% of acute myelogenous leukemia (AML) and up to 33% in AMLs with normal karyotypes [11], 56% of central and periosteal cartilaginous tumors [12], and 10-20% of cholangiocarcinomas as well as several rare cases of paraganglioma, colon cancer, prostate cancer, and lung cancer [13-17].

The role of an *IDH1* or *IDH2* mutation as an indicator of progression and survival is not well established. It has been reported that *IDH1/2* mutation results in decreased prognosis for AML [18-20] and increased prognosis for both low grade gliomas (65

months for mutant *IDH1/2* versus 38 months for wild type) and secondary GBMs (31 months for mutant *IDH1/2* versus 15 months for wild type) [2]. However, it is possible that *IDH1/2* mutant tumors may become clinically apparent earlier than *IDH1/2* wild type tumors, resulting in a misleading association with increased survival.

### *IDH1 enzymatic function and consequences of mutation*

Wild type IDH catalyzes the oxidative decarboxylation of isocitrate to  $\alpha$ -KG with simultaneous reduction of NADP<sup>+</sup> [21-23]. IDH1 mutations affect a single amino acid residue, R132 [1, 2], whereas IDH2 mutations affect two residues, R140 or R172 (the functional equivalent of R132 in IDH1) [11]. The most common *IDH1* mutation in tumors is the R132H missense mutation [2]. These recurrent IDH1/2 mutations result in two enzymatic changes: decreased wild type IDH function (oxidative decarboxylation of isocitrate to  $\alpha$ -KG with simultaneous reduction of NADP<sup>+</sup>) [21-23] and gain of a new enzymatic capability [(reduction of  $\alpha$ -KG to D-2-hydroxyglutarate (2-HG)] with simultaneous oxidation of NADPH [21, 22] (Figure 1.1). At the biochemical level, changes in the active site of mutant IDH1/2 enzymes prime the enzyme to produce 2-HG by increasing its affinity for  $\alpha$ -KG and shifting the conformation of the enzyme to favor an intermediate transition state [24].

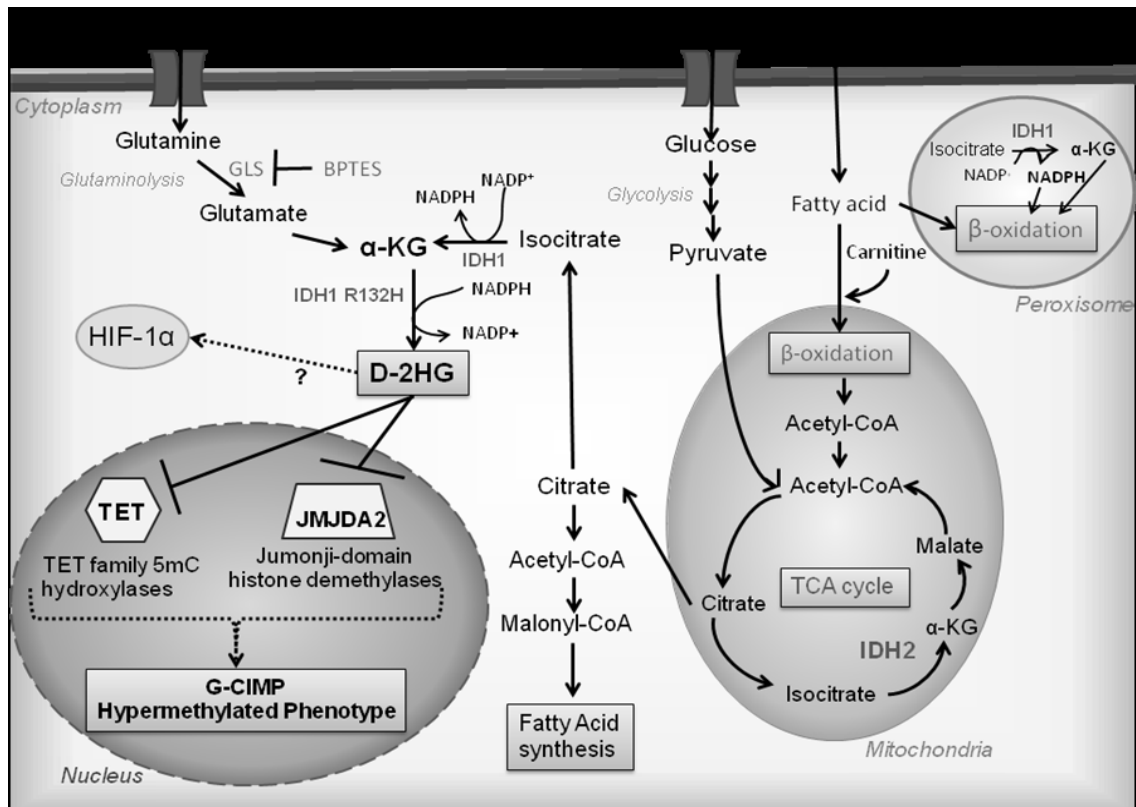


**Figure 1.1. Epigenetic and metabolic alterations in *IDH1/2* mutant tumor cells.** *IDH1/2* mutant enzyme activity results in high intracellular D-2-HG levels and alterations in glutamine metabolism, citrate and acetyl-coA levels, and fatty acid metabolism. D-2-HG is also able to compete with  $\alpha$ -KG for binding to histone demethylases and DNA hydroxylases likely contributing to a hypermethylated phenotype.

### *IDH1/2 mutations, 2-HG & metabolic disorders*

2-HG accumulation is a biochemical hallmark of IDH1/2 mutant tumors. Cells expressing wild type IDH1/2 have low levels of 2-HG, a normal byproduct of L-hydroxylysine breakdown that has no known function within the cell. 2-HG is normally removed from the cell through conversion to  $\alpha$ -KG by D-2-hydroxyglutarate dehydrogenase. Interestingly, D-2-HG and its stereoisomer L-2-HG accumulate in the metabolic disorders D-2 or L-2 hydroxyglutaric aciduria (D-2 or L-2-HGA), respectively [25-28].

L-2-HGA results from inactivation of L-2-hydroxyglutaric dehydrogenase [27], while D-2-HGA results from inactivation of D-2-hydroxyglutarate dehydrogenase or *IDH2* mutations [25, 27, 29]. Inherited *IDH2* mutations that cause D-2-HGA disease are identical to those found in gliomas or AML. Interestingly, L-2-HGA patients have been documented to develop gliomas, [29-33] however no cases of glioma have been documented in D-2-HGA patients, despite D-2-HG accumulation [25, 27, 28, 34]. These results may suggest that increased D-2-HG levels alone are not sufficient to cause tumorigenesis.

### *IDH1/2 mutations & Tumorigenesis*

*IDH1/2* mutations are predicted to have a very high probability of being driver mutations using CHASM (Cancer-Specific High-Throughput Analysis of Somatic Mutations) [35], which predicts the impact of the mutation on the protein, and attempts to determine the similarity of alteration with known cancer drivers. *IDH1/2* mutations occur in grade II progressive gliomas, prior to their progression to higher grade and

accumulation of the full complement of mutations found in glioblastoma . The frequency of these mutations does not increase with tumor grade, suggesting that these mutations are likely involved in the initial tumor development [2, 36]. Initially, studies suggested that *IDH1/2* mutations contribute to tumorigenesis through stabilization of HIF-1 $\alpha$ , similar to SDH and FH mutations [23]. These studies suggested  $\alpha$ -KG levels were significantly decreased in IDH1/2 mutant cells and that this decrease lead to inactivation of PHD2 and stabilization of HIF-1 $\alpha$  [23]. However, subsequent studies have found that  $\alpha$ -KG levels are not significantly altered in IDH1/2 mutant cells, despite increased cellular demand for D-2-HG production [21, 22, 37-39]. Additionally, studies in AML and glioma with IDH1/2 mutations did not detect increased stabilization of HIF-1 $\alpha$  [36, 40]. Therefore, while HIF-1 $\alpha$  stabilization could in theory could contribute to tumorigenesis, other pathways appear to play a larger role (Figure 1.1).

In cells that harbor *IDH1/2* mutations, intracellular 2-HG levels can reach up to 10 mM [21, 22, 41]. 2-HG and  $\alpha$ -KG are similar in structure, and recent studies have shown that 2-HG serves as competitive inhibitor of enzymes that utilize  $\alpha$ -KG as a co-factor (Figure 1.2) [40, 42].

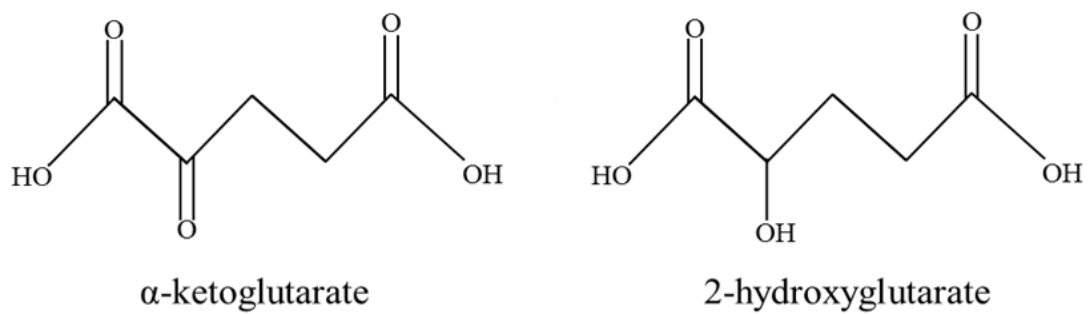


**Figure 1.2. Comparison of the structure of  $\alpha$ -ketoglutarate and 2-hydroxyglutarate.**



More than 60 enzymes utilize  $\alpha$ -KG as a co-factor [43] and 2-HG can competitively inhibit many of these enzymes. For example, 2-HG outcompetes  $\alpha$ -KG for binding to several classes of histone demethylases, PHD2 and the TET family of 5-methylcytosine hydroxylases [40, 42]. Crystallographic studies confirm that 2-HG fits into binding sites for  $\alpha$ -KG in dual-specificity histone demethylase KIAA1718 (KDM7A), factor inhibiting hypoxia-inducible factor (FIH) and jumonji domain containing protein 2A (JMJD2A) [40, 42]. High intracellular levels of 2-HG in IDH1/2 mutant tumors are likely sufficient for potent enzymatic inhibition and suggest a likely mechanism by which IDH1/2 mutations contribute to tumorigenesis [40].

Interestingly, mutant *IDH1/2* cases in AML have a characteristic hypermethylated phenotype which may result from inhibition of TET2 by 2-HG [44]. TET2 catalyzes the conversion of methylcytosine to 5-hydroxymethylcytosine and is mutated in approximately 24% of secondary AMLs. *TET2* mutations result in a hypermethylated phenotype highly similar to that seen in mutant *IDH1/2* AMLs, although the two mutations are mutually exclusive [44]. Differentially methylated genes in *IDH1* mutant gliomas include processes known to contribute to tumor progression as well as several metabolic pathways (Table 1). In gliomas, a hypermethylated phenotype has also been identified, the glioma-CpG island methylator phenotype (G-CIMP) which correlates tightly with *IDH1* mutations. Recent studies have shown that *IDH1* mutations alone are capable of inducing the G-CIMP phenotype as well as decreasing levels of 5-hydroxymethylcytosine in human astrocytes. Collectively, the data suggests that *IDH1*

mutations contribute to tumorigenesis by inducing wide scale epigenetic remodeling leading to altered gene transcription that favors neoplasia [45].

**Table 1.1. Pathways potentially altered by *IDH1/2* mutations in glioma**

Alteration	Tissue Studied	Hypomethylated pathways	Hypermethylated pathways
<b>Methylation</b>	IDH1 mutant gliomas	Methane metabolism	Protein kinase A signaling
		Pregnane X receptor/ Retinoid X receptor activation	Angiopoetin signaling
		Retinol metabolism	Ras related nuclear protein signaling
		Phenylalanine metabolism	Retinol transport
		Starch and sucrose metabolism	Cell cycle regulation
		Pentose and glucuronate interconversion	Methylated-DNA-protein-cysteine methyltransferase (MGMT)
		Androgen and estrogen metabolism	Fatty acid binding
<b>Transcription</b>	G-CIMP positive gliomas	<b>Increased</b>	<b>Decreased</b>
		Transcriptional regulation	Polysaccharide binding
		Nucleic acid synthesis	Heparin binding
		Metabolic processes	Glucosaminoglycan binding
		Cadherin based cell adhesion	Collagen
		Zinc finger transcription factors	Thrombospondin
			Cell morphogenesis
	Retinoic acid signaling		
	Fatty acid binding		
<b>Metabolism</b>	<i>IDH 1/2</i> mutant cells or cells treated with D-2HG	<b>Increased</b>	<b>Decreased</b>
		D-2-HG	NAAG
		Glycerol-3-Phosphate	NAA
		Glycerol-2-Phosphate	2-methyl butyryl carnitine
		Glycine	isobutyl carnitine
		Asparagine	$\alpha$ -aminoadipate
		Glutamine	Phosphocholine
		Serine	Propionylcarnitine
		Theroinine	Malate
		Phenylalanine	Fumarate
		Tyrosine	Citrate
		Tryptophan	
Methionine			

### *IDH1/2 mutations and metabolic alterations*

Transcriptional analysis of aberrantly methylated genes in primary G-CIMP tumors by Noushmehr, *et al.* found significant upregulation in genes involved in metabolic processes including carbohydrate metabolism, oxidative stress response, and nucleic acid synthesis (Table 1.1) [46]. Pathways transcriptionally repressed in G-CIMP tumors include those involved in tumor invasion, extracellular matrix remodeling, retinoic acid signaling and mesenchymal markers (Table 1.1) [46]. Subsequent studies using large sets of *IDH1* mutated low grade glioma samples as well as human astrocytes expressing *IDH1* mutant protein show that the *IDH1* mutation leads to methylation changes in genes regulating cellular differentiation, particularly the polycomb complex 2 (PRC2)-targeted loci [45]. Although the precise mechanism for these changes are not yet known, it is believed that 2-HG produced by *IDH1/2* mutations leads to global epigenetic alterations leading to changes in the expression of genes regulating cellular differentiation and metabolism.

Numerous metabolic changes have been confirmed by metabolomics studies on *IDH1/2* mutant cells [38, 39]. Reitman *et al.* identified changes resulting from expression of mutant *IDH1/2* or treatment with 2-HG (Table 1.1) [38]. Some metabolic alterations were found under both conditions; however, approximately half of the observed changes in *IDH1/2* mutant expressing cells could not be replicated by treatment with exogenous 2-HG. Most notably, decreases in glutamate levels and metabolites whose synthesis involves glutamate were not replicated by 2-HG treatment. Therefore, these changes are a direct result of the enzymatic activity of *IDH1/2* mutant enzymes.

One such metabolic alteration is the reduction of the neuropeptide N-acetyl-aspartyl glutamate (NAAG) and its precursor N-acetylated aspartic acid (NAA) in IDH1/2 mutant cells and tumors by up to 50-fold [38]. NAAG is synthesized from NAA and glutamate by NAAG synthase and functions in glutamatergic pathways of the brain [47]. Reitman *et al.* found that even when NAA levels are replenished, NAAG levels are not fully restored indicating that the glutamate necessary for generation of NAAG may be shuttled for production of  $\alpha$ -KG and subsequently 2-HG. In either case, the consequences of lowered intracellular NAAG levels on tumor formation and maintenance are unknown and warrant further study.

Mutant IDH1/2 produce 2-HG from glutamine derived  $\alpha$ -KG, resulting in increased flux through this pathway [22]. Therefore, cells expressing mutant IDH1/2 may be more dependent upon this pathway for growth and survival. In support of this hypothesis, inhibition of  $\alpha$ -KG synthesis from glutamine led to a 15-20% decrease in growth for cells expressing mutant IDH1 [39]. To further characterize this growth inhibition, metabolite levels were evaluated following treatment with BPTES, a small molecule inhibitor of glutamine, the first enzyme in the synthesis of  $\alpha$ -KG from glutamine. Glutaminase inhibition lowered glutamate and  $\alpha$ -KG levels in IDH1 wild type and mutant cells but 2-HG levels were not reduced, indicating the presence of a compensatory mechanism [39].

Changes in other metabolites following BPTES treatment also supported this hypothesis. These metabolic changes, including increases in glycolytic intermediates and decreased levels of TCA cycle intermediates, were seen in both wild type and mutant IDH1 expressing cells treated with BPTES [39]. Consequently,  $\alpha$ -KG might be produced

or diverted away from the TCA cycle to compensate for inhibition of  $\alpha$ -KG produced from glutaminase. In light of these results, metabolic inhibition has been suggested as a potential approach for selective targeting of *IDH1/2* mutant tumors. However our subsequent preclinical studies indicated that glutaminase inhibition alone would not likely be sufficient as a therapeutic strategy due to compensatory routes of  $\alpha$ -KG production. Inhibition of these compensatory routes would likely be required for an effective therapeutic response.

Changes in fatty acid metabolism may also result from the expression of *IDH1/2* mutants. Mutant *IDH1*-expressing cells exhibit decreased levels of citrate compared with wild type expressing *IDH1* cells, as well as increases in acetyl-CoA and triglyceride and phospholipid precursors [38, 39]. The combination of decreased citrate and increased lipid precursors may indicate that *IDH1* mutant expressing cells shuttle citrate out of the TCA cycle to produce lipids required for cell growth. Increases in fatty acid/lipid synthesis are a common characteristic of many cancers, including gliomas [48], and it is possible *IDH1/2* mutation may contribute to this phenotype. In addition, mutant *IDH1* may lead to decreased fatty acid oxidation in two ways: reducing available cofactors for peroxisomal  $\beta$ -oxidation and by decreasing carnitine biosynthesis for mitochondrial fatty acid transport.

Oxidation of  $\alpha$ -phytanic acids and  $\beta$ -oxidation of certain fatty acids within peroxisomes requires both NADPH and  $\alpha$ -KG, products of wild type *IDH1* activity. *IDH1* has been shown to be the sole source of these molecules within the peroxisomes [49]. Mutant *IDH1* has decreased ability to produce NADPH and  $\alpha$ -KG suggesting that mutation of *IDH1* may lead to decreased levels of these substrates within peroxisomes

and potentially decreased rates of fatty acid oxidation. Chowdury *et al.* demonstrated that high levels of 2-HG can inhibit  $\gamma$ -butyrobetaine hydroxylase 1, the last enzymatic step in carnitine biosynthesis [40]. Carnitine is required for activation and transport of fatty acids into the mitochondria to undergo  $\beta$ -oxidation. Consistent with this finding, levels of propionylcarnitine (a carnitine ester which sustains endogenous carnitine pools) were decreased in IDH1/2 mutant and 2-HG treated cells [38]. Therefore, IDH1/2 mutations may contribute to tumorigenesis by priming cells for growth by increasing fatty acid synthesis and reducing oxidation of certain fatty acids.

#### *IDH1/2 mutations and anti-cancer metabolism-based therapy*

The discovery of mutations in *IDH1* and *IDH2* in gliomas has profound implications for the understanding and treatment of these cancers. Studies in AML have shown that 2-HG can be detected in serum, and increased 2-HG levels correlate with *IDH1/2* mutational status [21, 41]. Elevated 2-HG levels could therefore serve as a biomarker to identify *IDH1/2* mutational status or monitor tumor growth or treatment efficacy. The use of 2-HG as a biomarker in gliomas is currently under investigation; however, detection may be technically challenging as the degree of 2-HG diffusion from solid glial tumors into serum, cerebrospinal fluid, or urine is unknown. Alternatively, 2-HG can be detected by magnetic resonance spectroscopy (MRS), allowing for non-invasive monitoring of tumor progression or classification of *IDH1/2* mutational status [50].

The distinct metabolic alterations resulting from IDH1/2 mutations reveal a potential opportunity for therapeutic intervention. One potential strategy for treatment of

IDH1/2 mutant tumors is inhibition of  $\alpha$ -KG synthesis from glutamine. Studies from our group have demonstrated that inhibition of this pathway can specifically slow the growth of mutant IDH1 expressing cells [39]. However, compensatory mechanisms and the mutational background of glioma cells suggest that multiple metabolic components may need to be targeted for the development of a successful therapeutic strategy. Further investigation of the role of *IDH1/2* and 2-HG on the epigenome and the metabolome will likely reveal additional targets.



## **CHAPTER 2**

### **DEVELOPMENT AND CHARACTERIZATION OF A NOVEL MODEL OF A PATIENT-DERIVED *IDH1* MUTANT GLIOMA WITH ALTERNATIVE LENGTHENING OF TELOMERES**

#### **Introduction**

Since the identification of *IDH1* as an oncogene in 2008, mutations have been found in the majority of grade II-III gliomas and secondary glioblastoma multiforme. Driver mutations in *IDH1* affect a single residue, R132, which is located in the substrate binding pocket. Mutations in this residue enhance the conversion of  $\alpha$ -ketoglutarate ( $\alpha$ -KG) to D-2-hydroxyglutarate (2-HG). Though normally present at very low levels in the cell, intracellular 2-HG concentrations can be increased up to 10-30 mM in *IDH1* mutant tumors [22, 41, 51]. Owing to the close structural similarity between the metabolites, 2-HG is believed to promote tumorigenesis by competitively inhibiting  $\alpha$ -KG dependent dioxygenases including the Jumonji C-domain containing histone demethylases and the TET family of DNA methylcytosine dioxygenases, believed to function in DNA demethylation [42]. Ultimately, continued exposure to 2-HG results in widespread cellular changes, including characteristic hypermethylation of genomic DNA, suppression of cellular differentiation and metabolic deficits [39, 45, 46, 52].

Although our understanding of *IDH1* mutated gliomas grows, the development of relevant models remains a challenge. Patient-derived *IDH1* mutant tumors have been difficult to culture and published xenografts are restricted to oligodendroglioma and oligoastrocytoma backgrounds [53, 54]. The development and molecular characterization

of additional endogenous *IDH1* mutant astrocytoma models is important for preclinical testing molecular based therapies which target progressive gliomas.

Here we report the generation of an endogenous patient derived *IDH1*-mutant anaplastic astrocytoma *in vivo* model, derived from a patient tumor with driver mutations in *TP53*, *CDKN2A* and *ATRX*. Although cells from this tumor do not proliferate *in vitro*, the *in vivo* model faithfully resembles the patient tumor and robustly expresses the IDH1 (R132H) mutant protein in both the flank and orthotopic sites. Additionally, the model exhibits a phenotype characteristic of an anaplastic astrocytoma characteristic including robust production of 2-HG, genome hypermethylation and alternative lengthening of telomere (ALT).

## **Material and Methods**

### **Xenograft establishment**

Tumor tissue was obtained during the resection of an anaplastic astrocytoma (WHO grade III) from a male patient. The tissue was mechanically dissociated, mixed with an equal volume of growth factor–reduced Matrigel (BD Biosciences, CA), and injected subcutaneously into the flanks of athymic nude mice (0.2cc/flank). All animal protocols and procedures were performed in accordance with the Johns Hopkins Animal Care and Use Committee guidelines. The mice were housed in standard facilities and given free access to Baltimore City water and chow. Animals were monitored frequently for signs of tumor growth. Xenografts were passaged in a similar fashion. Cross-sectional samples were obtained at each passage and either snap frozen or fixed in formalin. The samples were then embedded in paraffin and stained by H&E or used for immunohistochemistry. The *IDHI* (R132H) mutation was validated by direct sequencing at every passage.

For orthotopic xenografts, flank xenografts were resected and enzymatically dissociated using a 2:1 ratio of collagenase (10mg/mL, Invitrogen, NY) and hyaluronidase (1000 units/mL, Sigma, MO). Cell number and viability was assessed using Trypan blue exclusion. For intracranial implantations, 500,000 cells were stereotactically implanted into the right frontal cortex of 4-6 week old female athymic nude mice (NCI-Frederick) as previously described [55]. Mice were sacrificed upon showing symptoms of distress and the brains removed and formalin fixed for subsequent gross pathological examination of tumor formation and immunohistochemistry.

### **Sequencing of *IDH1***

Genomic DNA was isolated from patient tissue and flank xenografts using the DNeasy Blood and Tissue Kit (Qiagen, CA) according to the manufacturer's instructions. PCR and sequencing was conducted as previously described [39] Briefly, 60 ng of genomic DNA was added to a standard PCR reaction to amplify a portion of exon 4 of *IDH1* (forward 5'- GTAAAACGACGGCCAGTTGAGCTCTATATGCCATCACTGC 3', reverse 5'- CAATTCATACCTTGCTTAATGGG-3') . The PCR product was purified using the QIAquick Gel Extraction Kit (Qiagen, CA) and submitted for sequencing (Genewiz, NJ) using targeted primers (forward 5'- CGGTCTTCAGAGAAGCCATT-3', and reverse 5'- GCAAAATCACATTATTGCCAAC-3')

### **Histology and Immunohistochemistry**

All histopathological and immunohistochemical analyses were performed using tissue fixed in 10% formalin and embedded in paraffin. Tissue was obtained from patient samples after appropriate approval was obtained from the Johns Hopkins University Institutional Review Board. Paraffin-embedded sections were cut at 5 microns, deparaffinized, and stained with either hematoxylin and eosin (H&E) or immunohistochemical stains as specified. Heat-induced epitope retrieval was performed for 36 minutes at 98°C in EDTA buffer (pH 9.0). Immunohistochemical staining was performed using antibodies specific for IDH1 (R132H) (dilution 1:50, Dianova, clone H09, Germany) and visualized using the ultraView DAB detection system (Ventana Medical Systems, AZ).

## LC/MS

2-hydroxyglutarate levels were analyzed from snap frozen flank xenograft samples. Prior to extraction, frozen samples were thawed in a water bath at ambient temperature. Tissue homogenates were prepared at a concentration of 200 mg/mL in methanol. A 10  $\mu$ L aliquot of homogenized tissue was added to a borosilicate glass test tube (13x100 mm) containing 10  $\mu$ L of acetonitrile solution and 2-phosphonomethyl pentanedioic acid (1 mg/mL), which was used as the internal standard. The tube was mixed vigorously and evaporated under nitrogen gas at 4°C until completely dried. After the samples were dried, 100  $\mu$ L of acetonitrile and 100  $\mu$ L of N-tert-Butyldimethylsilyl-N-methyltrifluoro-acetamide were added sequentially. The tubes were incubated at 80°C for 1 hour then diluted 1:10 with acetonitrile. 100  $\mu$ L of the top layer was transferred to a 250- $\mu$ L polypropylene autosampler vial sealed with a Teflon crimp cap. 10  $\mu$ L of each sample was injected onto the LC/MS/MS for quantitative analysis using a temperature-controlled autosampling device operating at 10°C. Chromatographic analysis was performed using an ACQuity™ Ultra Performance LC (Waters, MA). Separation of the analyte from potentially interfering material was achieved at ambient temperature using X-Terra® RP18 column (20 x 2.1 mm, Waters, MA) packed with a 3.5  $\mu$ m RP<sub>18</sub> material (Milford, MA). The mobile phase used for the chromatographic separation was composed of acetonitrile with 0.1% formic acid and 2mM ammonium acetate in water (80:20, v/v) and delivered using an isocratic flow rate of 0.3 mL/minute. The column effluent was monitored using a QTRAP<sup>R</sup> 5500 mass spectrometer (AB SCIEX, MA). The instrument was equipped with an electrospray interface, operated in a positive mode and controlled by the Analyst 1.5.1 software. The mass spectrometry was programmed to monitor the

following MRM's 491.0 → 359 for 2HG and 683.0 → 551.4 for the IS. Samples were quantified over the assay range of 0.02 to 2 µg/mL. The standard curve of ratio response (analyte peak area/IS peak area) vs. concentration was plotted using linear regression with 1/x weighting for the data analyzed.

### **Whole Exome Sequencing**

Genomic DNA was isolated from normal human whole blood and flank xenograft tissue as described above. gDNA fragmentation was performed with the Bioruptor (Diagenode, NJ), and size selection at 200 bp - 300 bp was carried out. The exomes of gDNA were captured using the SureSelect All Exon 50Mb Target Enrichment kit (Agilent, CA) according to the manufacturer's instructions. DNA captured was run on the HiSeq2000 platform (Illumina, CA) with version 5 chemistry and version 4 flow cells, according to the manufacturer's instructions, to generate 100-base paired-end reads. Reads in fastq format were initially processed with GATK to remove Illumina adaptor sequences and Phred-scaled base qualities of  $\leq 10$  (-QT 10). After GATK trimming step, reads were mapped using the Burrows-Wheeler Aligner (version 0.6.1) with a -q 20 setting for read trimming, which removes the 3' portion of reads from an alignment if it is below the quality threshold specified. The alignments (sai files) were used to generate SAM (Sequence Alignment/Map) paired-end read files. All SAM files were converted to BAM files then sorted BAM files with Samtools (version 0.1.18). PCR and optical duplicates and multiple reads likely to have been read from a single cluster on the flow-cell image were marked with Picard tools. Regions that needed to be realigned were identified using the GATK Realigner Target Creator. The reads covering localized indels

were realigned, and quality values were recalibrated using GATK. The GATK was also used to locate, filter and annotate variants. Somatic changes including point mutations and small indels were called based on comparison between the xenograft and control blood. All predicted deleterious mutations not existing in dbSNP were counted. Mean exonic coverage was calculated for all exonic baits in xenograft and control samples by GATK. The mean exonic coverage was subsequently normalized by average whole exome coverage of the sample. Individual case vs. control log<sub>2</sub> ratios were then calculated for all the exons in the data set and plotted. The presence of copy-number alterations was detected using a combined approach involving a set of statistical Wilcoxon signed-rank tests performed on a 500,000 bp sliding windows along the genome. Amplifications were defined as greater than 4 copies of the gene (case vs. control log<sub>2</sub> ratio greater than 8).

### **Telomere-specific FISH and microscopy**

Telomere-specific FISH was conducted as previously described [56, 57]. Briefly, deparaffinized slides were hydrated, steamed for 20 minutes in citrate buffer (Vector Laboratories, GA), dehydrated, and hybridized with a Cy3-labeled peptide nucleic acid (PNA) probe complementary to the mammalian telomere repeat sequence ([N-terminus to C-terminus] CCCTAACCTAACCTAA). As a positive control for hybridization efficiency, a FITC-labeled PNA probe having specificity for human centromeric DNA repeats (ATTCGTTGGAAACGGGA; CENP-B binding sequence) was also included in the hybridization solution [58]. Slides were imaged with a Nikon 50i epifluorescence microscope equipped with X-Cite series 120 illuminator (EXFO Photonics Solutions Inc.,

Ontario, CA) and appropriate fluorescence excitation/emission filters. Grayscale images were captured for using Nikon NIS-Elements software and an attached PhotometricsCoolsnapEZ digital camera, pseudo-colored and merged. The telomerase-independent alternative lengthening of telomeres (ALT) phenotype was confirmed by the presence of abnormally large and intense intra-nuclear telomere FISH signals; a hallmark of cells utilizing the ALT pathway. Such foci are not observed in normal cells, nor are they observed in ALT-negative cancer cells, and thus serve as specific biomarkers of ALT.



## **Results and Discussion**

### **Establishment and serial passage of an IDH1 (R132H) anaplastic astrocytoma model**

Tumor was obtained from the resection of a recurrent anaplastic astrocytoma (WHO grade III) from a male patient with a history of glioma, presenting with a large right temporal lobe tumor. The patient had been diagnosed with a low grade astrocytoma (WHO grade II) twelve years prior, which had been surgically resected at that time. The recurrent tumor was found to have a high degree of anaplasia but lacked areas of necrosis and vascular proliferation. Direct sequencing of *IDH1* exon 4 demonstrated that the tumor harbored a heterozygous G395A (R132H) mutation (Figure 2.1C). This alteration was validated by detection of the mutant protein by immunohistochemistry (Figure 2.1B). Tumor tissue was implanted subcutaneously into athymic nude mice. Additionally, neurosphere culture was attempted in multiple media conditions including serum-free media containing hFGF and hEGF. Although the tissue was not amenable to *in vitro* culture, a first generation tumor arose in the mouse approximately one month after implantation as a large, localized subcutaneous mass. Direct sequencing of the xenograft tissue revealed retention of the *IDH1* (G395A) mutation but a loss of the wild type allele (Figure 2.1C). Immunohistochemistry demonstrated strong IDH1 (R132H) expression throughout the xenografted tissue (Figure 2.1B). All subsequent serial xenograft passages have retained the hemizygous IDH1 (R132H) mutation and exhibit robust expression of the mutant protein.

### **Xenografts show histopathological similarity and diffuse growth pattern**

Histopathological analysis of H&E samples obtained from the primary tumor sample and tumor-derived xenograft tissue show that both the flank and orthotopic xenografts maintain histopathological similarity to the primary tumor and also maintain morphology characteristic to an anaplastic astrocytoma (Figure 2.1B, Figure 2.2). The primary tumor was a cellular infiltrating astrocytoma with scattered gemistocytic cells as well as rare tumor giant cells. Scattered mitotic figures were identified consistent with the diagnosis of an anaplastic astrocytoma (Figure 2.2, inset). Immunostaining for mutant IDH1 was strongly and diffusely positive. Initial flank xenografts maintained many of the features of the primary tumor including a typical astrocytic morphology as well as scattered tumor giant cells, mixed with vascular, stromal, and skeletal muscle elements characteristic of this anatomical site (Figure 2.1).

Intracranial implantation of the tumor resulted in infiltrative growth throughout the cortex and deep grey matter structures (Figure 2.2). In some xenografts tumors, cells infiltrated through the corpus collosum to the contralateral hemisphere, a characteristic finding of infiltrating gliomas. Some xenografts grew within the leptomeninges and ventricles. As in the primary tumors, such growth was quite cellular with scattered mitotic figures and scattered tumor giant cells consistent with the original diagnosis of anaplastic astrocytoma (Figure 2.2, inset). While some gemistocytic features were noted within the intracranial xenograft, these were less prominent in the primary tumor.

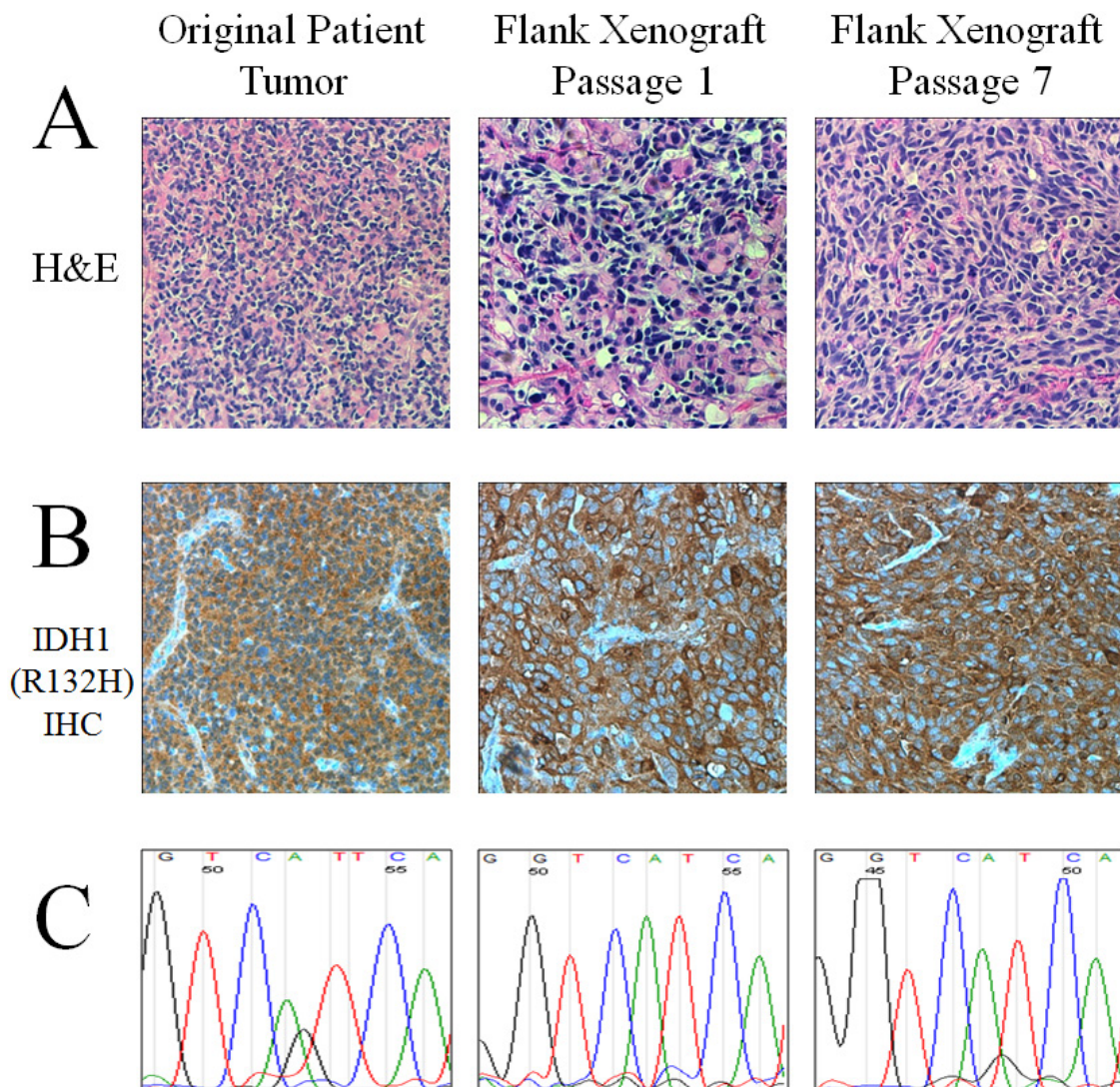


**Figure 2.1. Characteristic histological and genetic features of the IDH1 (R132H) anaplastic astrocytoma model.** (A) H&E sections of the primary tumor and subsequent flank xenografts show histopathological similarity to the original tumor including a typical astrocytic morphology, gemistocytic cells and mitotic figures. (B) Immunohistochemical staining specific for the IDH1 (R132H) mutant protein shows robust staining in the original tumor and all subsequent xenografts. (C) Sequencing of exon 4 of IDH1 shows an initial heterozygous G/A mutation in the original patient tumor which converts to a hemizygous genotype when the wild type copy is lost in the xenograft.

H&E

IDH1 (R132H)

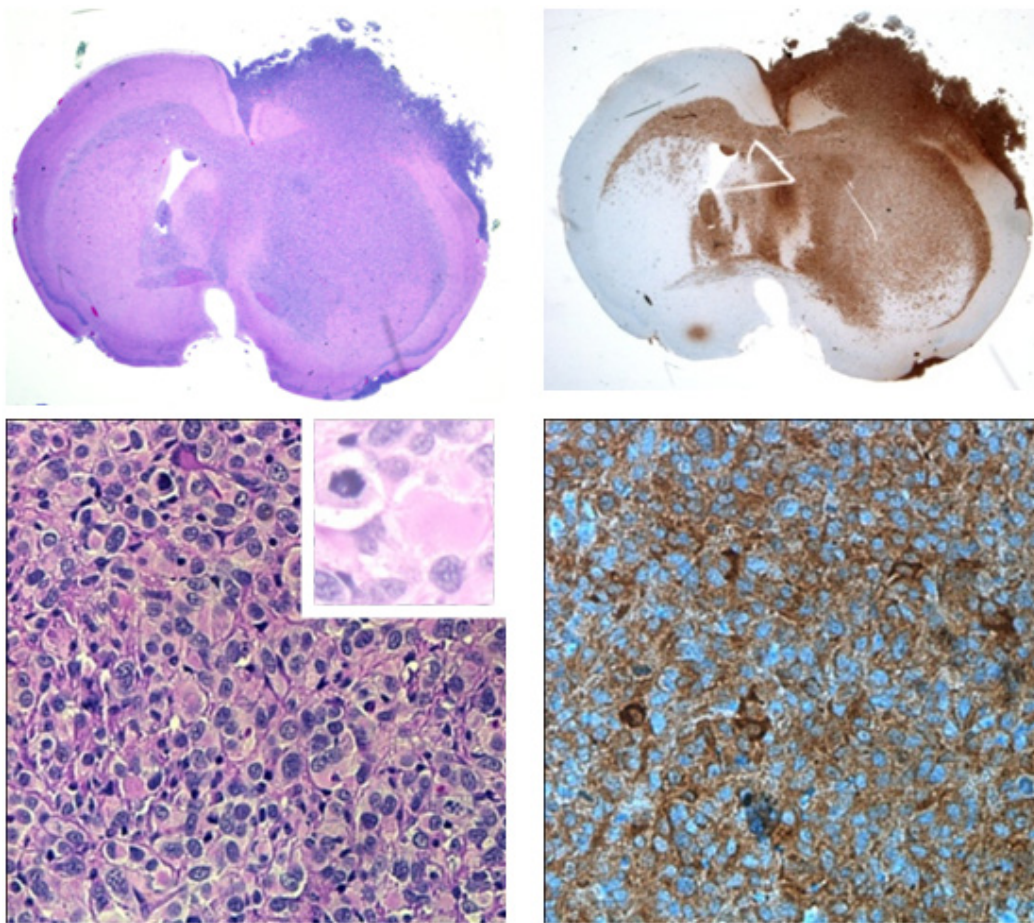


**Figure 2.2. Infiltrative growth pattern of orthotopically implanted JHH-273.** Sections of orthotopically implanted tumor stained with H&E (left) or by immunohistochemistry using an IDH1 (R132H) specific antibody (right) to show diffuse infiltrative growth pattern *in vivo*. Below, higher magnification sections show histopathological similarity including a typical astrocytic morphology with gemistocytic cells and mitotic figures (inset).

### ***IDH1* mutant model grows *in vivo* as flank and orthotopic tumors but not *in vitro***

The *IDH1* mutant xenograft grew rapidly in both the flank and at orthotopic sites (Figure 2.3). Serially transplantable flank xenografts reached maximum size (2.0 cm<sup>3</sup>) approximately 7 weeks after implantation and grew as dense, localized, hypercellular masses. Attempts to expand freshly dissociated flank tumor *in vitro* were unsuccessful, despite relatively high viability following dissociation. Since growth was observed *in vivo* but not *in vitro*, it is possible that there may exist a synergy between host environment and tumor cell culture. For this reason, co-culture was attempted using lethally irradiated mouse embryonic feeder cell in serum-free medium. However this was also unsuccessful.

Since *in vitro* culture was not possible, orthotopic implantation required fresh dissociation of flank tumor, in the absence of serum or growth factors. Orthotopically implanted tumors maintain robust *IDH1* (R132H) expression and a diffuse growth pattern, characteristic of anaplastic astrocytomas. Mice lost weight and showed neurological deficits approximately 5 weeks following implantation. Median survival time for mice bearing intracranial tumors was 63 days following implantation. The model was uniformly lethal and the time to death has remained consistent between passages.

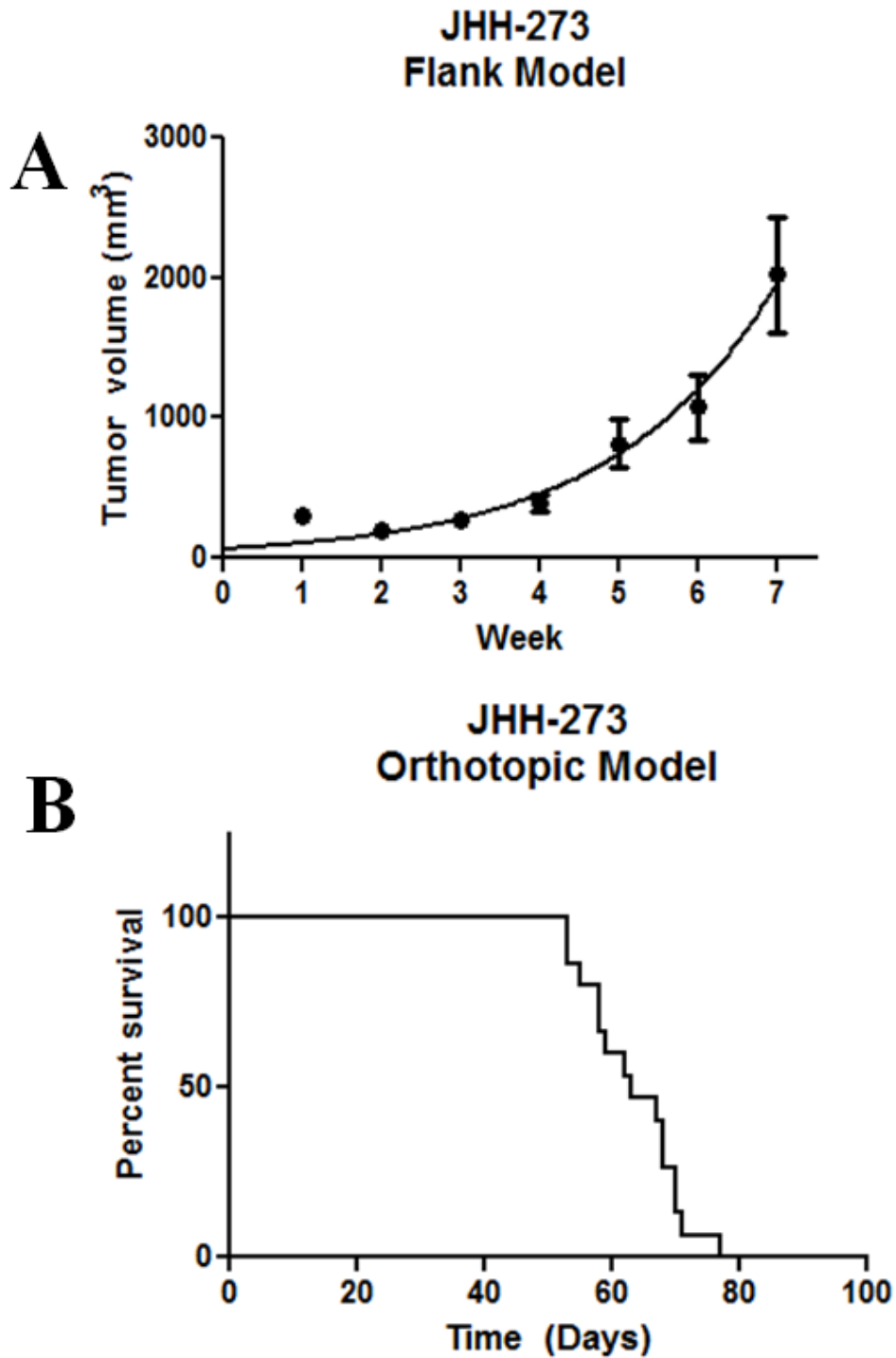


**Figure 2.3. Growth of JHH-273 *in vivo*** (A) Subcutaneously implanted flank xenografts grow to maximum size (2.0 cm<sup>3</sup>) in approximately 7 weeks. (B) Orthotopically implanted xenografts have a median survival time of 63 days and are uniformly lethal (n=15).

### **JHH-273 produces 2-HG**

Production of 2-HG from  $\alpha$ -KG is a hallmark of *IDH1* mutations and its accumulation is believed to underlie the pathogenesis of *IDH1* mutations. Therefore, we investigated whether our patient-derived model produces 2-HG. LC/MS analysis was performed on snap frozen tissue from well-established flank xenograft (passage 7). JHH-273 produced high levels of 2-HG which correspond to the endogenous levels reported in *IDH1/2* mutant gliomas (Figure 2.4). In contrast, 2-HG was nearly undetectable in tissue obtained from *IDH1* wild type glioma controls.

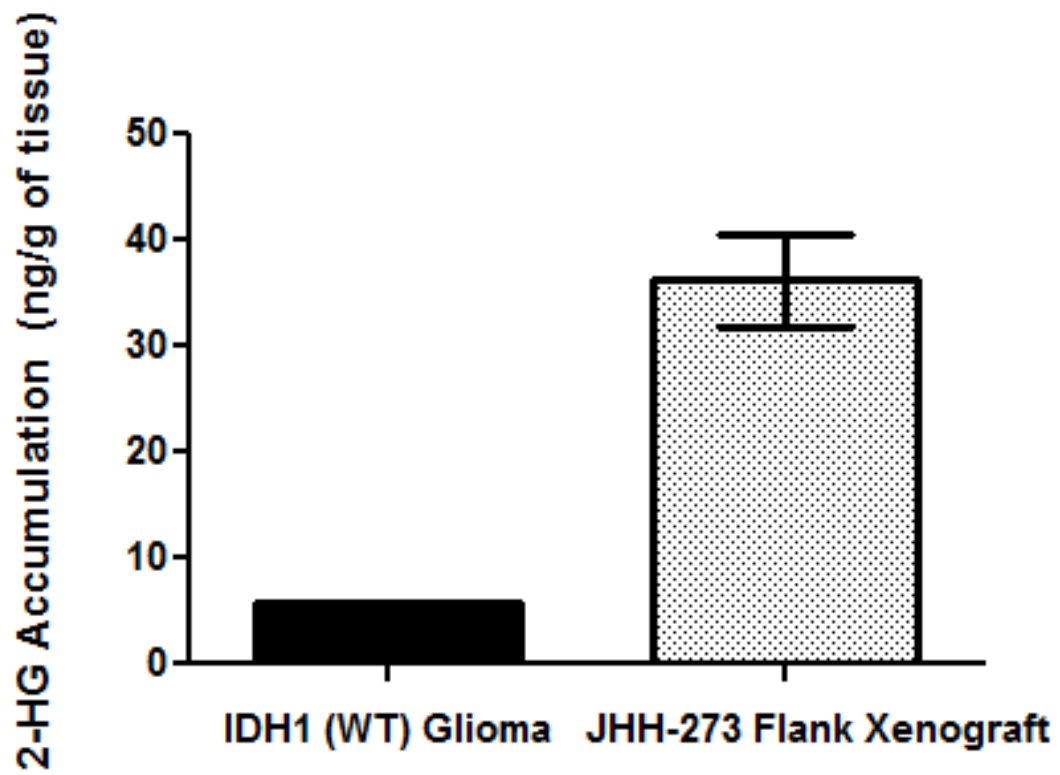


**Figure 2.4. 2-HG production in JHH-273. *IDH* mutant xenograft produces high levels of 2-HG as measured by LC/MS. Error bars=SEM**



## **Whole exome sequencing reveals mutations in *TP53*, *ATRX*, and deletion of *CDKN2A***

To more completely characterize our *IDH1* mutant model, we performed whole exome capture and next-generation sequencing on gDNA obtained from flank xenograft tissue. Although matched control DNA was not available for analysis, we utilized gDNA derived from the whole blood of two unrelated individuals as well as the dbSNP database to remove common SNPs. We achieved a mean coverage of 124x across the exome, with 94% covered by at least 10x. Copy number variation (CNV) analysis revealed deletion of genetic content at multiple points throughout the genome, resulting in a loss of 39 known genes and including a 1.3 Mb deletion in chromosome 9. No genetic amplifications were observed. After removal of common SNPs, our analysis revealed 231 candidate somatic mutations in 170 genes. These mutations consisted of missense (83.1%), frameshift (7.4%), splice site (3.0%), nonsense (0.9%), and insertions/deletions (5.6%).

Promising candidate mutations were selected based on a comprehensive list of known driver gene mutations [59]. Of the 125 published Mut-driver genes, five were present in the *IDH1* (R132H) model. Exome sequencing confirmed the known *IDH1*, and additionally revealed missense mutations in *TP53*, a frameshift mutation in *ATRX* and deletion of *CDKN2A* (Table 2.1). The frameshift mutation in *ATRX* is predicted to produce an early stop codon, resulting in the loss of 81% of the protein. Concurrent mutations in *TP53*, *IDH1*, *CDKN2A* and *ATRX* have been well reported in multiple anaplastic astrocytoma samples and have been used as genetic signatures in the classification of glioma. Whole exome sequencing thus demonstrated that our *IDH1*

(R132H) model bears a mutant profile consistent with *IDH1* mutant anaplastic astrocytoma.

**Table 2.1. Genetic Mutations in JHH-273**

<b>Gene Symbol</b>	<b>Genetic Mutation</b>	<b>Mutation Type</b>	<b>Protein Mutation</b>
<i>ATRX</i>	T1635X	Frameshift	Nonsense
<i>CDKN2A</i>	N/A	Deletion	N/A
<i>IDH1</i>	G395A	Missense	R132H
<i>TP53</i>	C736T	Missense	E246L
<i>TP53</i>	C619T	Missense	M207V

### **Model exhibits Alternative Lengthening of Telomeres (ALT)**

Due to the association of *ATRX* mutations with the alternative lengthening of telomeres phenotype, telomere length was assessed by telomere specific fluorescent *in situ* hybridization (FISH) in primary tumor, and in flank and orthotopic xenografts. An ALT positive phenotype was identified by the presence of large ultra-bright telomeric FISH foci in a subset of tumor cells [60]. The primary patient tumor exhibited ALT-associated foci (Figure 2.5A), which was robustly maintained in the flank and orthotopic xenografts (Figure 2.5B and C, respectively). Interestingly, although the original patient sample showed ALT-associated foci only in a subset of the tumor cells, the flank and orthotopic xenograft had a more homogenous pattern, with nearly every cell being positive for ALT-associated foci. In contrast, the ALT phenotype was not present in an *IDH1* wild type glioma patient sample (Figure 2.5D).

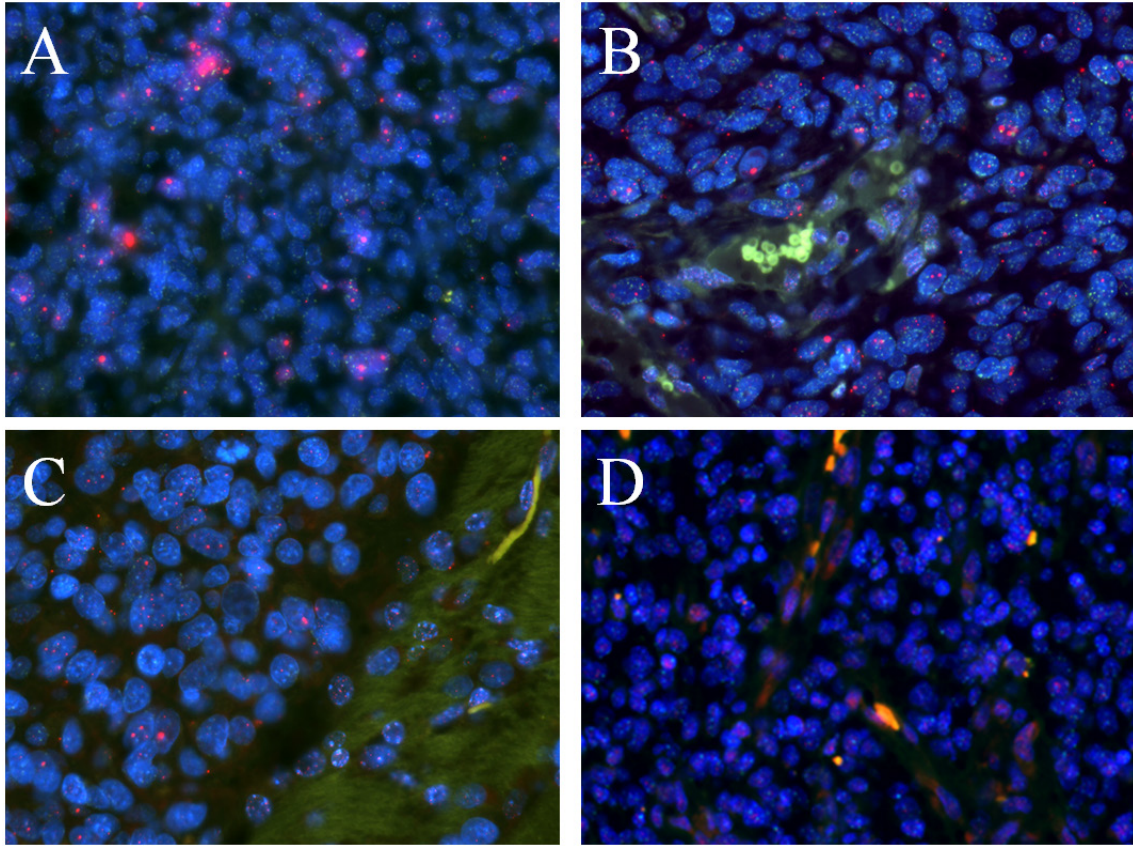


**Figure 2.5. ALT characterization in JHH-273.** (A) Telomere-specific FISH analysis in the original patient tumor, (B) the flank xenograft tumor (C) and the orthotopically implanted tumor show a strongly ALT positive phenotype, as indicated by large, ultrabright telomere FISH signals. D. *IDH1* wild type GBM is ALT negative.

## Conclusions

In this work, we characterize the first *in vivo* model of a patient-derived *IDH1* mutant anaplastic astrocytoma, JHH-273, which was originally reported in a preclinical drug study earlier this year. The model was established after many attempts in order to enhance translational studies with more accurate *in vivo* models. Prior work from our laboratory showed that the JHH-273 model maintains the *IDH1* mutation after serial passage, produces 2-hydroxyglutarate *in vivo*, and bears a hypermethylated phenotype characteristic of *IDH1* mutant gliomas [61]. Further genetic sequencing revealed that the JHH-273 model harbors mutations in *TP53*, *CDKN2A* and *ATRX*, and exhibits the ALT telomere maintenance phenotype. The JHH-273 model maintains infiltrative intracranial growth with a consistent time to death, making it the only practically usable animal model for *IDH1*-mutant anaplastic astrocytoma. This model represents the only documented *IDH1*-mutant anaplastic astrocytoma model with ALT, and only the third documented glioma model with ALT, making this model useful for preclinical studies targeting the ALT pathway [60, 62]. Collectively this data suggests that the patient derived JHH-273 model is characteristic of an *IDH1* mutant anaplastic astrocytoma and represents a valuable tool for preclinical testing of compounds targeting *IDH1* mutations or ALT and for investigating this distinct molecular subset of gliomas.

## **CHAPTER 3**

### **5-AZACYTIDINE REDUCES METHYLATION, PROMOTES DIFFERENTIATION AND INDUCES TUMOR REGRESSION IN A PATIENT-DERIVED *IDH1* MUTANT GLIOMA XENOGRAFT**

#### **Introduction**

Abnormal DNA hypermethylation has been recognized as a possible target in cancer and DNA methylation reducing drugs, including 5-azacytidine that was reported nearly 40 years ago [63]. 5-azacytidine is an analogue of cytidine and it is incorporated into DNA and RNA. At therapeutic doses, 5-azacytidine inhibits DNA methyltransferase leading to a reduction in DNA methylation. In particular, 5-azacytidine is a potent inhibitor of DNA methyltransferase 1 (DNMT1), inducing ubiquitin-dependent degradation of the protein [64].

Unfortunately, despite the growing understanding of *IDH1/2*-mutant gliomas, the development of effective therapies has proved challenging. *IDH1/2*-mutant tumors do not adapt to growth in culture and endogenous mutant models remain scarce [53, 65]. Engineered cell lines have been useful in elucidating the complex network underlying *IDH1/2* mutations but lack the appropriate genetic and mutational context, as well as the microenvironmental context, found in patient derived *IDH1/2*-mutant gliomas. Patient derived endogenous *IDH1/2*-mutant models are therefore critical for the development and testing of therapies which target *IDH* oncogene-driven pathways and mechanisms.

Here we report preclinical demonstration of efficacy and mechanism of 5-azacytidine in our anaplastic astrocytoma model (Chapter 2). Long term administration of 5-azacytidine resulted in inhibition of DNMT1, loss of methylation of key genomic

markers, *in vivo* induction of differentiation, reduction of cell proliferation and significantly reduced tumor growth. Tumor growth was essentially arrested at 14 weeks and subsequently showed no signs yet of re-growth after withdrawal of therapy.



## **Materials and Methods**

### **Flank xenograft establishment and passage**

A fresh tissue sample was obtained during the resection of an anaplastic astrocytoma (WHO grade III) from a male patient as described in Chapter 2.

### **Sequencing of IDH1**

DNA isolation and sequencing of *IDH1* exon 4 was performed as described in Chapter 2.

### **Histology and Immunohistochemistry**

Histology and immunostaining was performed as described in Chapter 2.

### **Pyrosequencing of target genes**

Bisulfite conversion was carried out using EpiTect Bisulfite Kit (Qiagen, CA) with 1µg genomic DNA. PCR was carried out using PyroMark PCR kit (Qiagen, CA) following the manufacturer's instructions. The samples were run in a 25 µL reaction with 2.5 µL of primer reconstituted according to manufacturer's instructions. The thermocycler conditions are an initial activation step of 95°C for 15 minutes, 45 cycles of 94°C for 30 seconds, 56°C for 30 seconds, and 72°C for 30 seconds, and a final extension of 72°C for 10 minutes. Controls included 100%, 50%, and 0% human methylated control DNA (Zymo Research Corp, CA), and a no-template control. Samples plus controls were amplified using primer kits Hs\_PYCARD\_03\_PM, Hs\_RBP1\_02\_PM, Hs\_MGMT\_01\_PM, Hs\_SOX9\_08\_PM, and Hs\_BMP4\_02\_PM. Amplified DNA was

then pyrosequenced using the PyroMark CpG Assay kit (Qiagen, CA) on the PyroMark 24 system (Qiagen, CA). Bisulfite conversion, PCR amplification and pyrosequencing was performed at the Genetic Resources Core Facility, Johns Hopkins Institute of Genetic Medicine, Baltimore, MD.

### **Therapeutic administration of 5-azacytidine to JHH-273 flank bearing mice**

Female, athymic nude mice aged 4-6 weeks were implanted with the JHH-273 tumor line as described above. Five days after implantation, mice received daily *i.p.* injections of 5-azacytidine (Sigma Aldrich, MO; 3 mg/kg) diluted in sterile water for five days followed by a two day rest period. Treatment continued until tumors reached maximum allowable size. Following sacrifice, tumors were harvested and passaged individually into another set of female athymic nude mice, identically as before. 5-azacytidine treatment was resumed immediately after tumor implantation and continued until tumors reached maximum allowable size (Cycle 2). Following the second cycle of treatment, tumors were again resected and passaged into two groups of mice. To assess the durability of the therapeutic response, 5-azacytidine treatment was withdrawn in one group of pre-treated animals and resumed immediately in the other. Treatment strategy is outlined in Figure 4. Tumors were measured weekly and volume was calculated as:  $H \times L \times W$  (mm<sup>3</sup>).

### **Immunoblotting**

Protein lysates were prepared using RIPA buffer and immunoblot analysis was performed as previously described [66]. Briefly, protein lysates were obtained from

freshly resected flank tumors using RIPA buffer (ThermoScientific, MA) containing Halt protease inhibitor cocktails (Pierce, IL) according to the recommendations of the manufacturer. Lysates (50 µg) were heated to 95°C in Laemmli sample buffer for 10 min and separated on SDS polyacrylamide gels. Proteins were transferred to polyvinylidene fluoride membranes (Bio-Rad) in Western transfer buffer [25 mmol/L Tris (pH 8.3), 192 mmol/L glycine, and 20% methanol]. For Western blot analysis, membranes were blocked for 1 h at room temperature in 5% nonfat dry milk in TBST (1× TBS, 0.1% Tween 20) and incubated overnight at 4°C with antibodies against GFAP (Cell Signaling Technology, MA), or DNMT1 (New England Biolabs, MA). After washing, membranes were incubated with a horseradish peroxidase-linked goat anti-rabbit antibody for 1 h at room temperature. Antibody detection was achieved by chemiluminescence according to the manufacturer's recommendations (Pierce, IL).

### **Statistical analysis**

Statistical analyses were performed using a student t-test for comparisons between the treatment groups. A p value of < 0.05 was considered significant.

## Results

### JHH-273 CpG hypermethylation and by 5-azacytidine treatment *in vivo*

Recent data has shown that one consequence of *IDH* mutation is the induction of global DNA hypermethylation that is believed to contribute to tumor formation and maintenance [45, 52, 67, 68]. In order to determine the methylation status JHH-273, we performed pyrosequencing analysis of bisulfate-converted genomic DNA at five genetic loci. This technique allows the identification of bases that are methylated *in vivo* (reference). Targets were selected based on the reported frequency of hypermethylation in *IDH1* (R132H) primary tissue and engineered cell systems as well as their known functional impact in tumorigenesis or tumor maintenance [37, 45, 68-76]. The analysis was performed using genomic DNA obtained from both early and late passage xenograft tissue (passages 1, 7 and 10) as well as two unrelated *IDH1* (R132H) anaplastic astrocytoma samples and three *IDH1* (WT) glioma primary patient samples as controls.

The original patient tumor exhibited high degrees of CpG methylation at four of the five loci, which was maintained in the xenograft tissue at all passages analyzed (Figure 3.1A). The high levels of CpG methylation were consistent with other primary patient *IDH1* (R132H) anaplastic astrocytoma samples. In contrast, wild type *IDH1* gliomas exhibited low levels of methylation at all targets analyzed, consistent with reported data. Of note, although *SOX9* hypermethylation in *IDH* mutant gliomas has been reported in several studies, we did not detect significant methylation in either primary tissue sample or xenograft. Overall, JHH-273 reflected the hypermethylated genomic landscape of the original patient tumor and exhibited the characteristics of an *IDH1* (R132H) anaplastic astrocytoma.

To determine whether the hypomethylating agent 5-azacytidine was able to reverse methylation of the JHH-273 tumors *in vivo*, we analyzed CpG methylation of flank tumors following treatment with one cycle of 5-azacytidine (1 mg/kg and 5 mg/kg). 5-azacytidine was able to substantially reduce CpG hypermethylation at four of the five targets analyzed in a dose specific manner (Figure 3.1B). Although a significant tumor regression was observed in the high dose treatment group, this dose was associated with significant toxicity (data not shown).

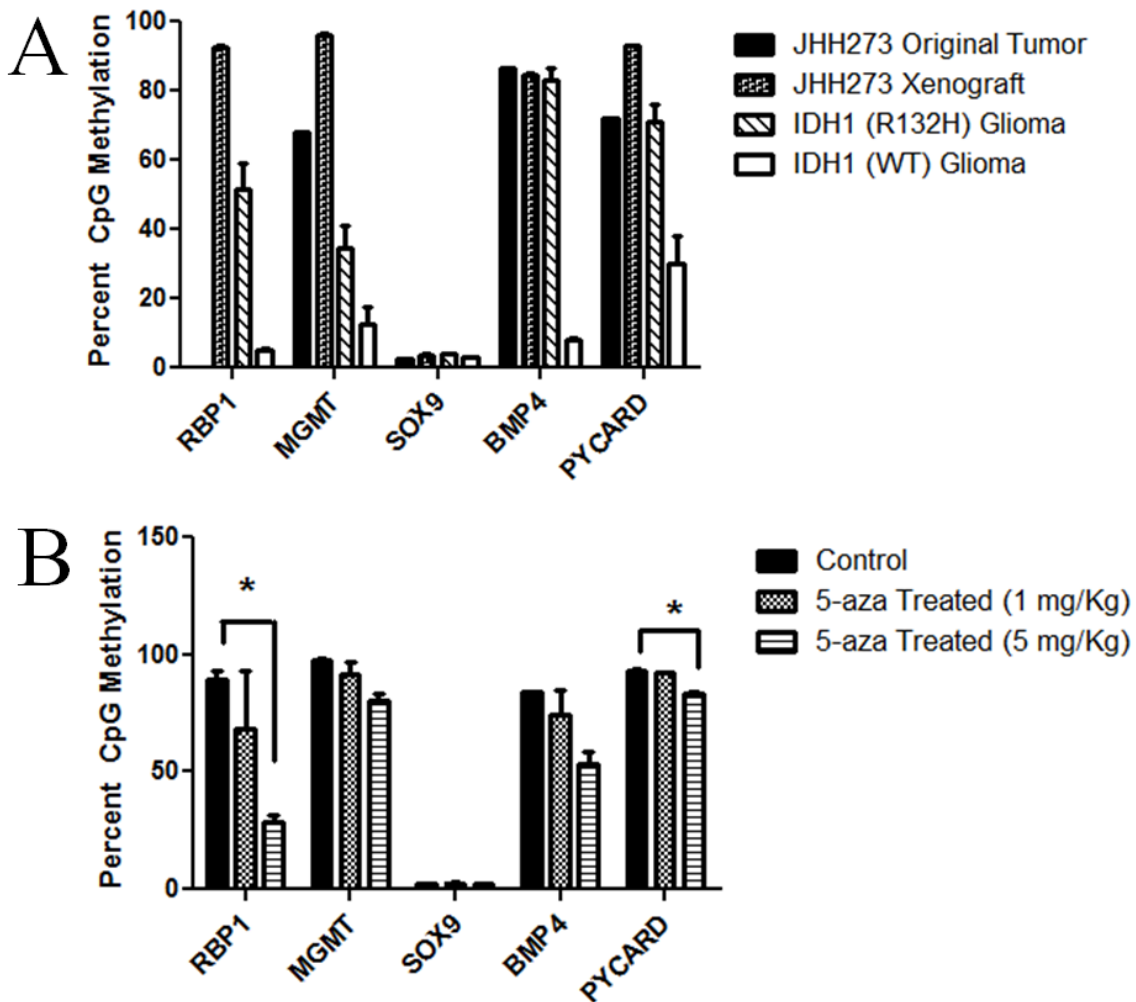


**Figure 3.1. JHH-273 shows characteristic DNA hypermethylation which can be reversed with 5-azacytidine treatment *in vivo*.** (A) Pyrosequencing shows that the original patient tumor exhibits high levels of DNA methylation in several target genes. This hypermethylated phenotype is maintained in the xenograft and is characteristic of *IDH1* mutant gliomas. In contrast, *IDH1* wild type glioma is not hypermethylated. (B) 5-azacytidine treatment for 1 cycle reverses methylation at several targets in a dose specific manner. \*  $p < 0.05$ , Error bars=SEM.

### **Long term treatment with 5-azacytidine reduces tumor growth in an IDH1 mutant model**

To extend the relative exposure time of JHH-273 tumor to 5-azacytidine, serial passage of flank tumors from treated mice was performed using the strategy outlined in Figure 3.2. A moderate reduction of tumor burden was observed within one treatment cycle, but this decrease was not statistically significant ( $p=0.27$ ) (Figure 3.5A). Following passage of 5-azacytidine treated flank tumors, a second cycle of treatment with the 5-azacytidine was continued until maximum tumor burden was reached. 5-azacytidine significantly reduced tumor burden by the fourth week of Cycle 2 ( $p<0.01$ ). This difference between untreated and treated tumors increased throughout the treatment period (Figure 3.3B). During passage of tumor after Cycle 2, the tissue was found to be unusually firm and encapsulated by gelatinous tissue. Enzymatically disassociated fractions of the tumor were found to contain fewer than 10% viable cells, by Trypan blue exclusion.

5-azacytidine serially treated tumors were implanted for a third time into two groups of athymic nude mice (Cycle 3). To assess the durability of the therapeutic response, treatment was withdrawn in one group. Significant tumor regression was observed in both groups, including the treatment withdrawn group, suggesting a durable therapeutic response of 5-azacytidine (Figure 3.3C).

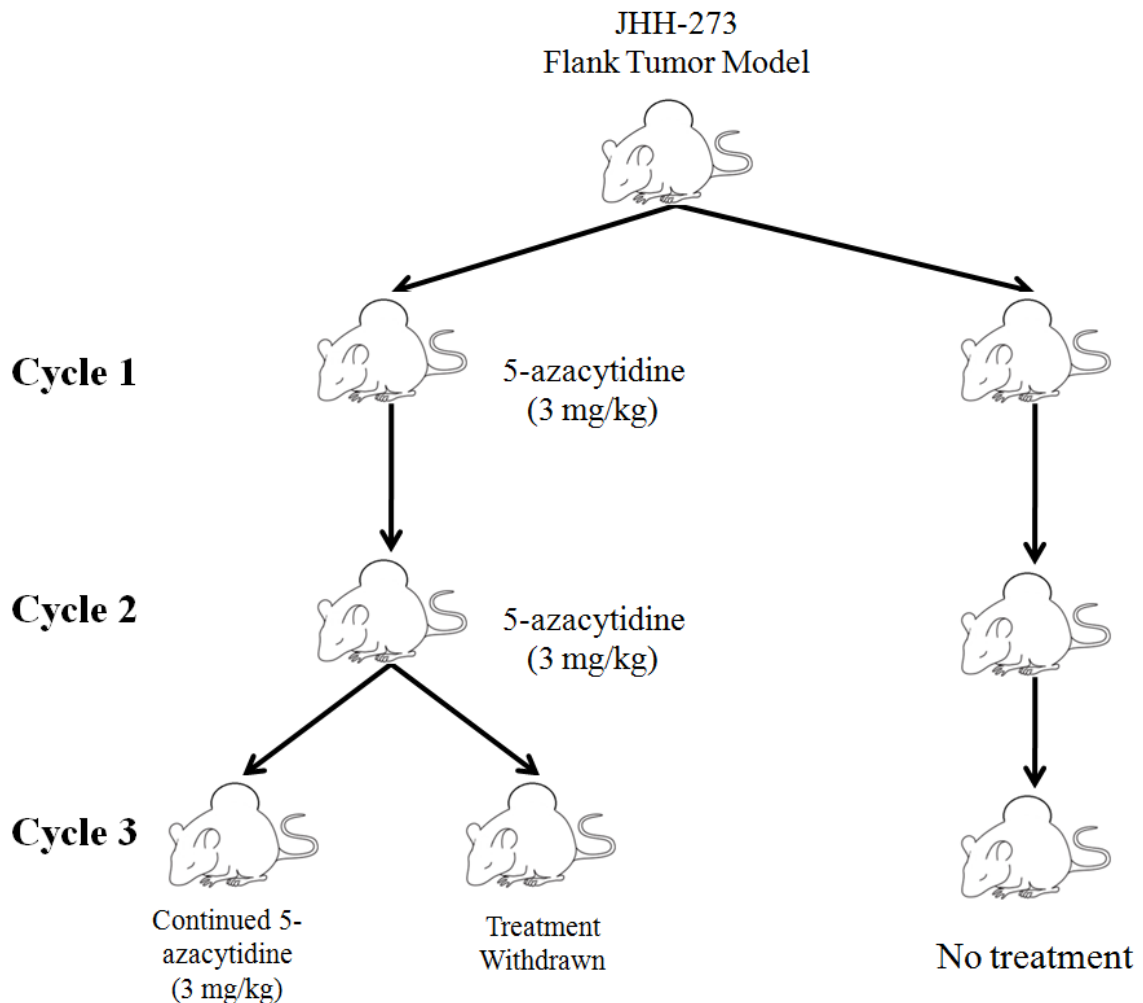


**Figure 3.2. Treatment strategy for 5-azacytidine in the IDH1 mutant flank model.** Flank tumors were treated with 5-azacytidine until maximum tumor size was reached (Cycle 1). In order to extend the relative time of treatment, the flank tumors were individually passaged and 5-azacytidine treatment resumed immediately following implantation (Cycle 2). Tumor passaging was repeated a third time into two groups, one which immediately resumed 5-azacytidine treatment or one which had treatment withdrawn (Cycle 3).



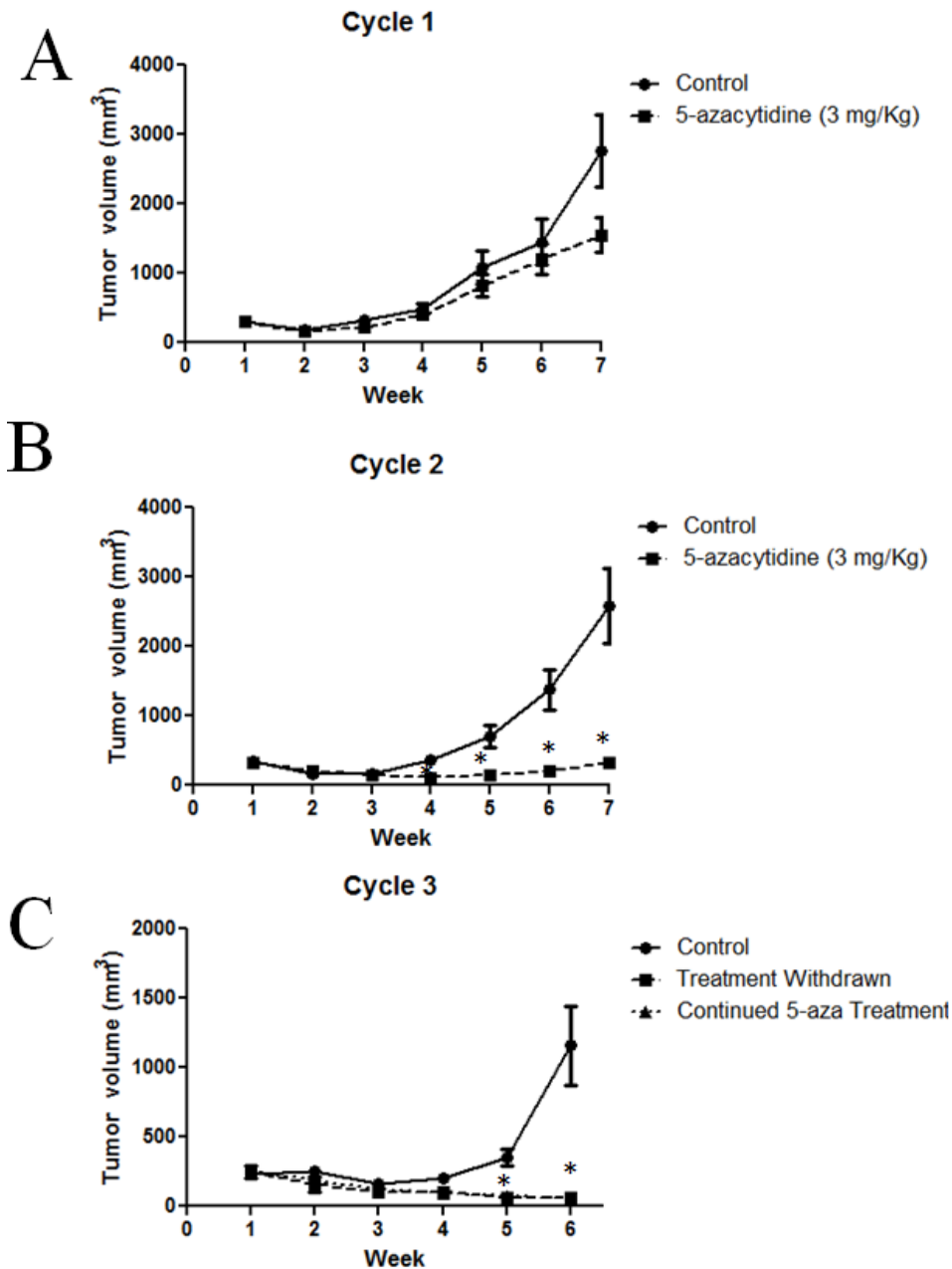


**Figure 3.3. Long term treatment with 5-azacytidine reduces tumor growth in an IDH1 mutant model.** (A) Mice bearing IDH1 mutant flank tumors and treated with 5-azacytidine show a reduction in tumor burden ( $p=0.27$ ) (B) Cycle 2 of 5-azacytidine treatment significantly reduces tumor growth compared to untreated tumors (C) Pre-treatment with 5-azacytidine significantly decreases tumor growth, even after treatment is withdrawn. Cycles 1 and 2: Five mice (10 tumors) per group, Cycle 3: Four mice (4 tumors) per group. \*  $p<0.01$ , Error bars=SEM

### **Treatment with 5-azacytidine induces differentiation and reduces the proliferative index**

Intracellular 5-azacytidine activity was confirmed by DNMT1 expression in tissue from untreated and 5-azacytidine treated tumors (Cycles 1 and 2). DNMT1 is expressed at high levels in untreated tumors but expression of the protein is robustly inhibited following treatment with 5-azacytidine. DNMT1 protein was undetectable after one treatment cycle of 5-azacytidine (Figure 3.4A).

Prior studies had proposed that the *IDH* mutation inhibits DNA and histone demethylation, leading to a block in cellular differentiation [69]. Additionally in a study published in this issue, treatment of endogenous *IDH1* mutant glioma cell lines with hypomethylating agent 5-aza-2'-deoxycytidine was found to drive differentiation *in vitro* [67]. To test whether reduction of hypermethylation by 5-azacytidine leads to an increase in cellular differentiation *in vivo*, immunoblotting was performed for glial fibrillary acidic protein (GFAP) in tumors treated with 5-azacytidine. GFAP expression was undetectable in the untreated tumors, confirming the undifferentiated phenotype of IDH (R132H) tumors. Following one cycle of 5-azacytidine treatment, GFAP expression was robustly increased and protein levels were maintained throughout the second treatment cycle. To validate these findings, immunohistochemical analysis was performed on formalin fixed paraffin embedded tissue. Compared with untreated tissue, 5-azacytidine treatment markedly increased the fraction of GFAP-positive cells (Figure 3.4B, 3.5A). These results confirm that IDH mutations plays an active role in repressing cellular differentiation, a deficiency which is reversible with long term treatment with hypomethylating agent 5-azacytidine.

To test whether 5-azacytidine-induced differentiation translated to a decrease in proliferation, tumors from 5-azacytidine treated mice were stained with the proliferation marker Ki-67. 5-azacytidine treatment significantly reduced the fraction of Ki-67 positive cells in a time dependent manner, with the greatest decrease in proliferation during the 7 to 14 week period of Cycle 2 (Figure 3.5B).

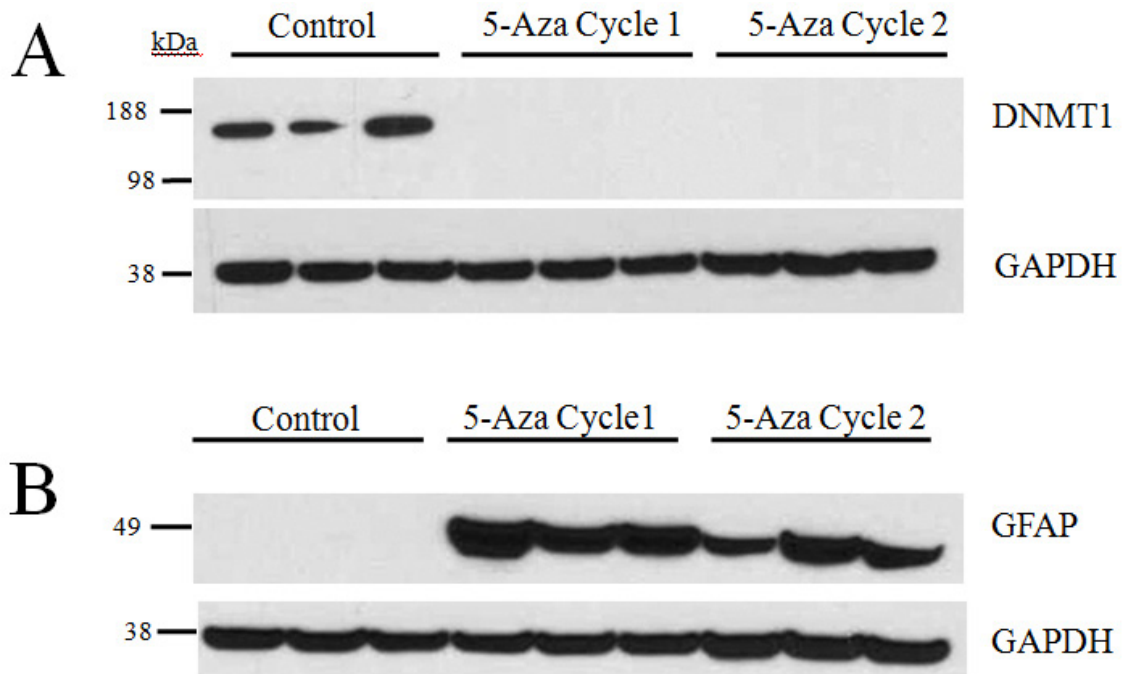


**Figure 3.4. Treatment with 5-azacytidine induces differentiation in an *in vivo* IDH1 (R132H) glioma model.** (A) 5-azacytidine treatment causes loss of DNMT1 expression *in vivo* following one treatment cycle. (B) GFAP expression is restored following one passage of 5-azacytidine treatment and is maintained.

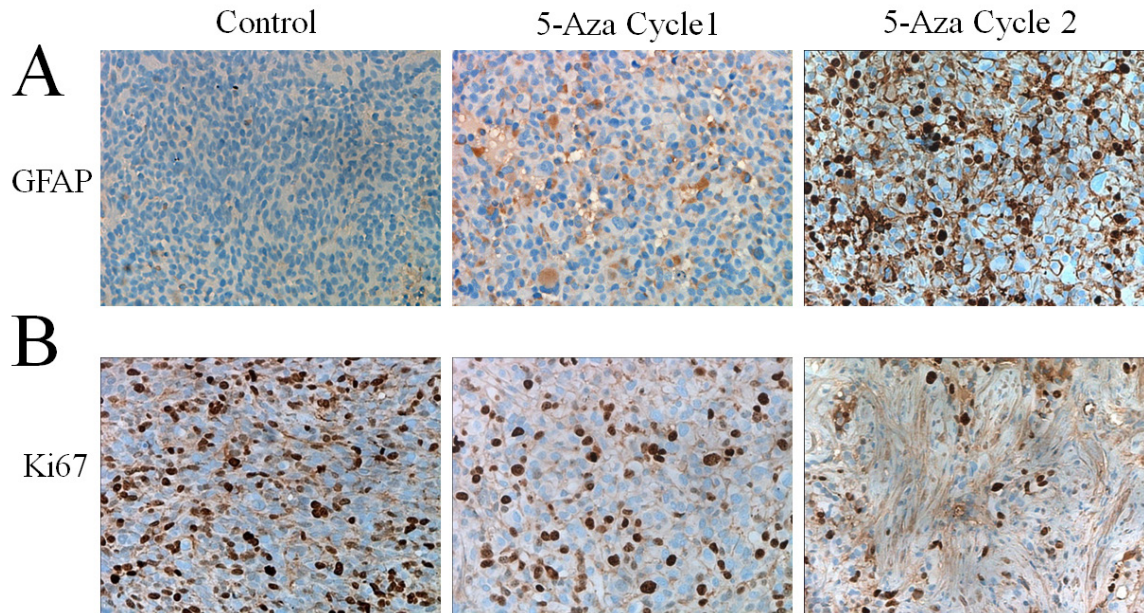


**Figure 3.5. Treatment with 5-azacytidine induces differentiation and reduces the proliferative index in an *in vivo* IDH1 (R132H) glioma model. (A)** Immunohistological staining of GFAP shows significant increase of protein expression in the cytoplasm of 5-azacytidine treated cells (B) Ki67 staining shows a decrease in the proliferative index of 5-azacytidine treated cells in a time dependent manner.

## Discussion

Somatic mutations in *IDH1* and *IDH2* are found in a high percentage of low grade and progressive gliomas. *IDH* mutant gliomas are associated with a pro-neural gene expression profile, a characteristic pattern of DNA hypermethylation and a signature of repressive histone methylation [52]. It is believed that the 2-HG produced by *IDH*-mutant proteins promote tumorigenesis by blocking cellular differentiation via hypermethylation of tumor suppressor genes involved in differentiation [44-46, 52, 68].

The current therapy for low grade gliomas is surgical resection followed by monitoring with periodic MRI scans. Unfortunately, most of these tumors recur or progress to high grade gliomas. If the gliomas progress to high grade no curative therapy is available, although repeat surgery and additional treatment with radiation can temporarily slow tumor growth. Median survival for grade II astrocytoma (fibrillary or diffuse astrocytoma) is approximately 5 to 7 years and for grade III astrocytoma (anaplastic), median survival is 4 to 5 years [77]. New therapies are urgently needed.

In this work, we report the first *in vivo* model of a patient derived *IDH* mutant anaplastic astrocytoma, JHH-273. This model was established after many attempts, which underscores the difficulty most labs have had at growing *IDH* mutant astrocytomas. The goal of establishing the xenografts was to enhance translational studies with more accurate models harboring relevant mutations that developed during the course of human tumorigenesis. Importantly, we show in that *IDH1* (R132H) expression is stable through multiple passages, 2-HG is robustly produced, and the model bears a hypermethylated CpG phenotype characteristic of an *IDH1* mutant glioma.

Once evidence emerged that hypermethylation was a likely oncogenic mechanism of *IDH* mutations, demethylating agents became an attractive choice for translational investigation. When 5-azacytidine treatment was first tested in the JHH-273 model, a decrease in methylation was observed in a dose specific manner but was associated with only marginal reduction of tumor burden. We were able to achieve a significant *in vivo* response by lowering drug dosing and extending the relative exposure time of tumor to drug by passaging pre-treated tumor tissue into treatment naïve mice.

Short term 5-azacytidine treatment (1 cycle, 7 weeks) perhaps started to slow tumor growth, but by doubling the treatment time, we were able to achieve tumor regression. Treatment with 5-azacytidine for 2 cycles elicited a durable treatment response, as treatment withdrawal for an additional 6 weeks did not produce any visible signs of tumor re-growth (although we continue to monitor the mice). At the end of 2 treatment cycles, the tumors had changed dramatically in appearance with the presence of hard fibrous tissue and less than 10% cell viability. Additionally, with 7 weeks of treatment 5-azacytidine drives cellular differentiation to the astrocytic lineage as seen by increase in GFAP expression, further underscoring the reversal of the presumed mechanism of mutant *IDH1* oncogenesis. These data are consistent with the hypothesis that demethylating drugs may promote re-expression of previously silenced Polycomb controlled genes and subsequently activate genes involved in differentiation [45, 78].

The observed induction of cellular differentiation and subsequent reduction in proliferation following treatment with a hypomethylating agent in *IDH* mutant glioma is surprisingly consistent with an independent study that was simultaneously reported [67]. In this companion work, decitabine, a closely related demethylating agent, was found to

preferentially induce differentiation in *IDH* mutant glioma cells but not in wild type cells. This work showed very similar mechanistic results to this study, and since both the drug and the models utilized are independent, the collective evidence supports the hypothesis that the gene expression reactivated by demethylating agents is sufficient to produce terminal differentiation in the self-renewing malignant cells of the tumor.

5-azacytidine is currently FDA approved for the treatment of myelodysplastic syndrome and well tolerated in patients. Its close structural analogue, decitabine, can effectively cross the blood brain barrier in laboratory animals [79]. Experimentally, pre-treatment of cells with transient, low dose exposure of 5-azacytidine to has been shown to decrease tumorigenicity and percentage of stem-like cells in several cancer models [80]. In addition to considering 5-azacytidine or decitabine for recurrent or high grade *IDH* mutant glioma, 5-azacytidine therapy may also be useful as a maintenance therapy following tumor resection. Due to the infiltrative growth pattern of astrocytoma, complete resection is nearly impossible and the remaining tumor frequently recurs, often as a higher grade glioma. Low-dose treatment with 5-azacytidine following resection may drive the remaining mutant *IDH* glioma cells into differentiation, thereby delaying recurrence.

This work supports the further investigation of demethylating drugs such as 5-azacytidine for its use against mutant *IDH1* gliomas both in the laboratory and in clinical trials. Although it is very likely that these drugs have the potential to help patients with *IDH1* mutant gliomas, the optimal demethylating drug, patient population, dosing strategy, delivery and drug combinations have yet to be determined.



## **CHAPTER 4**

### **FUTURE DIRECTIONS OF 5-AZACYTIDINE THERAPY FOR *IDH1* MUTANT GLIOMAS**

We have demonstrated tumor regression in our novel *IDH1* mutant model using the DNA methyltransferase 1(DNMT1) inhibitor 5-azacytidine (5-aza). The success of this strategy relied on the knowledge that *IDH1* mutant gliomas exhibit a phenotype of globally hypermethylated DNA and chromatin. 5-azacytidine is currently an FDA approved drug for the treatment of myelodysplastic syndrome and is well tolerated in patients. Its close structural analogue, decitabine (DAC, 5-aza-2'-deoxyazacytidine) has been shown to be effective at slowing tumor growth in *IDH1* mutant oligodendroglioma models [79]. Experimentally, pre-treatment of cells with transient, low dose exposure of 5-azacytidine has been shown to decrease tumorigenicity and percentage of stem-like cells in several cancer models [80]. Although it is very likely that these drugs have the potential to help patients with *IDH1* mutant gliomas, the optimal demethylating drug, patient population, dosing strategy, delivery for intracranial tumors and drug combinations have yet to be determined.

#### **Determine intracranial accumulation of 2-deoxy-5-azacytidine and 5-azacytidine in the orthotopic model.**

Studies have shown that 2-deoxy-5-azacytidine (DAC) has the ability to cross the blood-brain barrier and can accumulate in the cerebrospinal fluid up to half of its plasma concentration after drug infusion in dogs and rabbits [79]. However, the intracranial accumulation of 5-aza is not yet known. To determine intracranial accumulation of 5-aza,

non-tumor bearing mice were injected with 5-aza (3mg/kg) for 3 days upon which time the brains were harvested and snap frozen. Preliminary LC/MS optimization assays of the homogenized brains detected 5-aza at a concentration of approximately 0.5-0.8 ng/mg of tissue, although validation of these values will be necessary to determine precise intracranial concentrations. Additionally, the blood brain barrier is frequently compromised in cases of malignant glioma increasing the likelihood that these therapeutic compounds reach the target site. However, the intracranial accumulation of DAC and 5-aza has not yet been determined in tumor bearing animals. For this reason, it will be of clinical value to repeat this experiment using numerous concentrations of 5-aza and DAC to determine intracranial, intratumoral and plasma concentration at multiple points following injection. A standard curve can then be used to quantify the levels of drug in the brain to assess whether therapeutic levels can be obtained intracranially.

**Compare single agent efficacy of 2-deoxy-5-azacytidine and 5-azacytidine on the reduction of tumor burden and in orthotopic models.**

Preliminary data from our laboratory suggests that pretreatment with demethylation therapy significantly extends the survival of intracranially implanted *IDH1* mutant tumors (Figure 4.1).

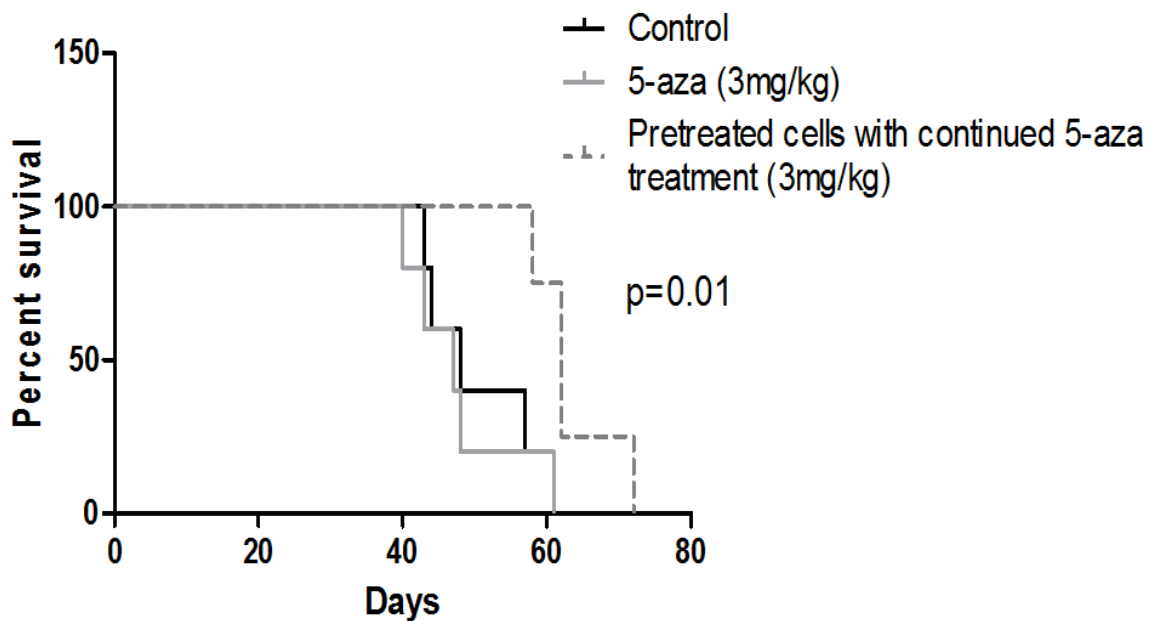


**Figure 4.1. Pretreatment of IDH1 mutant cells with 5-azacytidine extends survival in orthotopically implanted tumors.** Mice bearing flank tumors were treated with 5-Aza (3mg/kg) until maximum tumor size was reached. The flank tumors were dissociated and implanted intracranially. Treatment with 5-aza was resumed until the time of death. Pretreatment of tumors with 5-aza significantly extends survival compared to control mice and 5-aza treated mice which were bearing untreated tumors.

In this experiment, mice bearing flank tumors were treated with vehicle or 5-aza (3 mg/kg) until maximum tumor size was reached. The tumors were then resected and disassociated into single cell suspensions. The vehicle treated cells were implanted intracranially into two groups of mice, one which received then vehicle control and the other received 5-aza treatment (3 mg/kg). The 5-aza pretreated cells obtained from the flank tumors were implanted intracranially into a third group of mice which then received continued 5-aza treatment (3 mg/kg). When implanted intracranially, pretreatment of the *IDH1* mutant tumors significantly extended survival compared to the non-pretreated tumor and suggests that demethylation therapy may reprogram the epigenome to slow tumor growth. Although 5-aza alone did not extend survival in non-pretreated tumors, this is likely because the tumors grow too rapidly for a treatment effect, as is the case in the flank model. A slower growing *IDH1* mutant cell line will be necessary to determine the single agent efficacy of demethylating agents in non-pre-treated tumors. At the time of writing, we are currently conducting this experiment using the *IDH1* mutant oligoastrocytoma line BT142, a slower growing tumor which has a median survival of approximately 100 days [53]. Following implantation, mice are being treated with *i.p.* injections of 5-aza (2 mg/kg), DAC (0.5 mg/kg) or vehicle (saline). If one of the demethylating agents is successful in extending survival, we will then use an *IDH1* wild type glioma neurosphere line, developed in our laboratory, as a control to ascertain the specificity of the drug response to the *IDH1* mutation [55].

Although DAC is only approved for I.V. administration, 5-aza is approved in both subcutaneous and I.V. forms and in Phase III trials for oral administration. Additionally, there is now an approved generic for the subcutaneous 5-aza. For the drug which exhibits

the greatest extension of survival, it will be of clinical value to test all approved forms to determine the most effective mode of administration *in vivo*.

### **Optimize demethylation therapy with current standard of care**

Following primary tumor resection, the current available therapeutic options include ionizing radiation and oral administration of the DNA alkylating agent temozolomide (Temodar, TMZ). It has been found that methylation of the DNA repair gene O-6-methylguanine-DNA methyltransferase (*MGMT*) sensitizes tumors to killing by TMZ [81]. In order to determine whether demethylating agents would interfere with TMZ sensitization due to *MGMT* demethylation, mice bearing JHH-273 *IDH1* mutant flank tumors were treated with 5-aza or vehicle control until maximum tumor size was reached. Tumors were passaged to the flanks of mice, which subsequently received TMZ (50 mg/kg, 5 days). This data suggests that pretreatment of *IDH1* mutant tumors with demethylating agent 5-aza does not alter sensitivity to TMZ (Figure 4.2). However, this data will need to be validated in the JHH-273 intracranial model and in additional models of *IDH1* mutant glioma, such as BT-142.

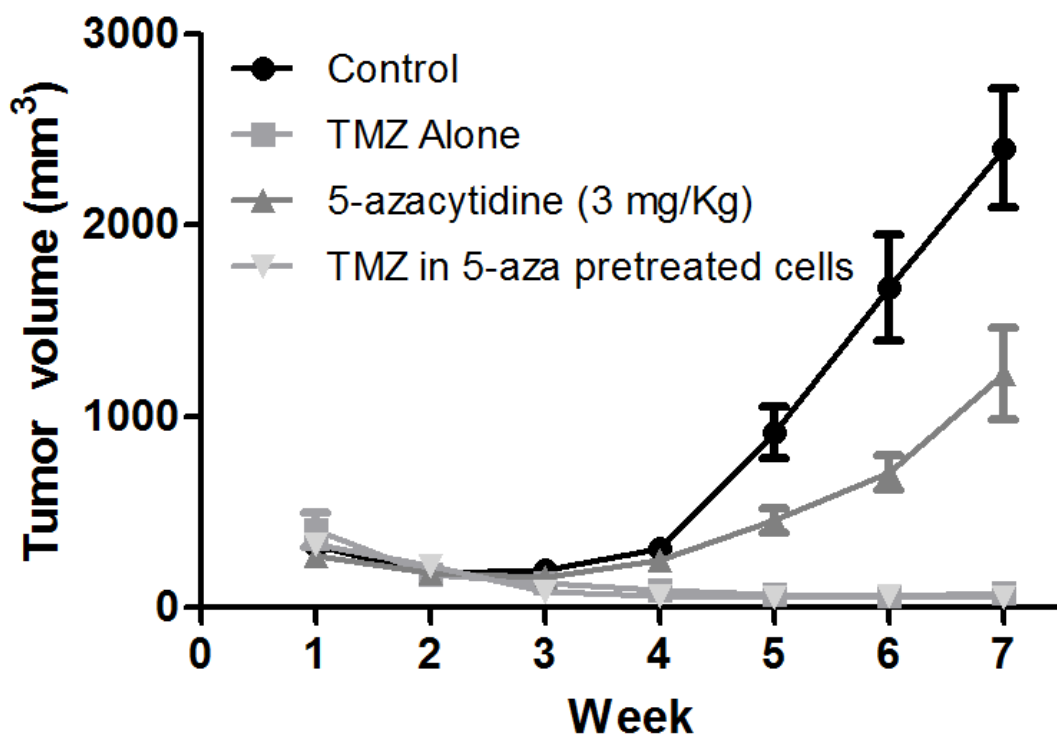


**Figure 4.2. 5-azacytidine pretreated tumors retain TMZ sensitivity *in vivo*.** Mice bearing flank tumors were treated with 5-azacytidine (3mg/kg, 7 weeks) or vehicle control. 5-aza and vehicle treated tumors were passaged into the flanks of mice which were then treated with TMZ (50 mg/kg, 5 days) or with 5-azacytidine. 5-azacytidine pretreated tumors retain sensitivity to TMZ. Error bars=SEM

Alterations in DNA methylation and chromatin structure by treatment with chromatin modifying agents or transfection with hypermethylated DNA fragments have been known to alter radiosensitivity of cells [82]. In a recent study, pre-treatment of the *IDH1* wild type U373MG glioblastoma cell line with DAC for 18 hours induced radiosensitivity compared to cells exposed to radiation alone [82, 83]. It will therefore be important to assess whether DNA demethylation will interfere or enhance ionizing radiation therapy in *IDH1* mutant gliomas *in vivo*. To conduct this experiment, a small animal irradiator may be used to provide 10 grays of localized radiation total over a period of 5 days (2 gy x 5). Mice bearing JHH-273 flank tumors will receive 5-aza (3 mg/kg) or vehicle until maximum tumor size is reached. Tumors will then be passaged to the flanks of mice, which will then receive localized radiation and tumor growth monitored by caliper volume measurements. Collectively, these experiments will greatly inform clinical trials by allowing us to determine the appropriate timing of demethylation therapy to the current standard of care.

### **Determine synergistic combinations with IDH1 Mutant Enzyme Inhibitors**

Since the discovery of mutant *IDH1* as an oncogene, the development of IDH1 inhibitors has been intensely pursued in industry and in academia. One such molecule, AGI-5198 (Agiros, MA) was identified by a high throughput enzymatic screen and found to potently inhibit the mutant enzyme and reduce 2-HG levels [84]. This inhibitor was able to induce demethylation of histone H3K9me3 and modestly increase expression of genes associated with differentiation. Although the reduction in tumor burden and DNA methylation was modest[67], combination with DNA demethylating agents is likely to

have a synergistic effect by allowing simultaneous reversal of pathogenic hypermethylation and suppression of further methylation by blocking 2-HG production.

Although the AGI-5198 compound is the only published mutant enzyme inhibitor, we are currently in negotiations with several pharmaceutical companies (GlaxoSmithKline, Novartis) and intend to accumulate (or synthesize from the patent literature) as many inhibitors as possible for testing *in vivo*. Because the blood brain barrier permeability of *IDH1*-mutant enzyme inhibitors is not yet known, it will be vital to determine single agent efficacy of mutant IDH1 enzyme inhibitors and combinations with DNA demethylating agents in both the flank and orthotopic model.

### **Combination therapy with HDAC inhibitors**

Due to the widespread epigenetic aberrations in *IDH1*-mutant glioma, modulation of additional epigenetic targets is likely to synergize with demethylation therapy (Figure 4.3). Widespread increases in repressive histone methylation occur in *IDH1* mutant gliomas due to the inhibition of JmjC domain containing histone demethylases by 2-HG [42]. This increase in repressive histone methylation in IDH1 mutants is followed by reduction of activating marks of histone acetylation [52], leading to transcriptional repression. Several histone deacetylase inhibitors (HDAC) and histone demethylase inhibitors have been developed, most of which are in clinical trials with two obtaining FDA approval for myeloma and lymphoma. Although these compounds exhibit single agent efficacy, substantial synergy has been found between DNA demethylating and histone modulating agents in multiple models [85-88].



Because *IDH1* mutant tumors exhibit reduced DNA acetylation and increased histone methylation, targeting each of these is likely have synergy with DNA demethylating agents *in vivo*. Vorinostat (SAHA) is the first HDAC inhibitor to gain FDA approval and is currently for the treatment of cutaneous T cell lymphoma. Recently, SAHA has shown synergy with decitabine to induce autophagy and inhibit cell growth in an ovarian xenograft model [89]. The combination of SAHA with 5-aza or DAC is currently in multiple clinical trials and the combination has shown strong activity in a Phase I trial of newly diagnosed cases of MDS or acute myelogenous leukemia and Phase II trials are currently underway [90].

Next generation HDAC inhibitors such as entinostat (MS-275) show additional promise for neoplastic malignancies with entinostat currently in phase II trials for Hodgkin's lymphoma, breast and lung cancer. Interestingly, entinostat was found to exhibit synergy is 5-azacytidine in an orthotopic model of lung adenocarcinma, leading to a reduction of tumor burden and re-expression of Polycomb regulated genes [91]. In clinical trials, the combination of entinostat and 5-aza was shown to have significant activity in relapsed non-small cell lung cancer [92]. We have found that the MS-275 is well tolerated in our *IDH1* mutant model and hypothesize that combinations of vorinostat or entinostat with DNA demethylation therapies (5-aza or DAC) will be synergistic in *IDH1* mutant gliomas due to the widespread epigenetic changes, both DNA and histone, which occur in these types of tumors.

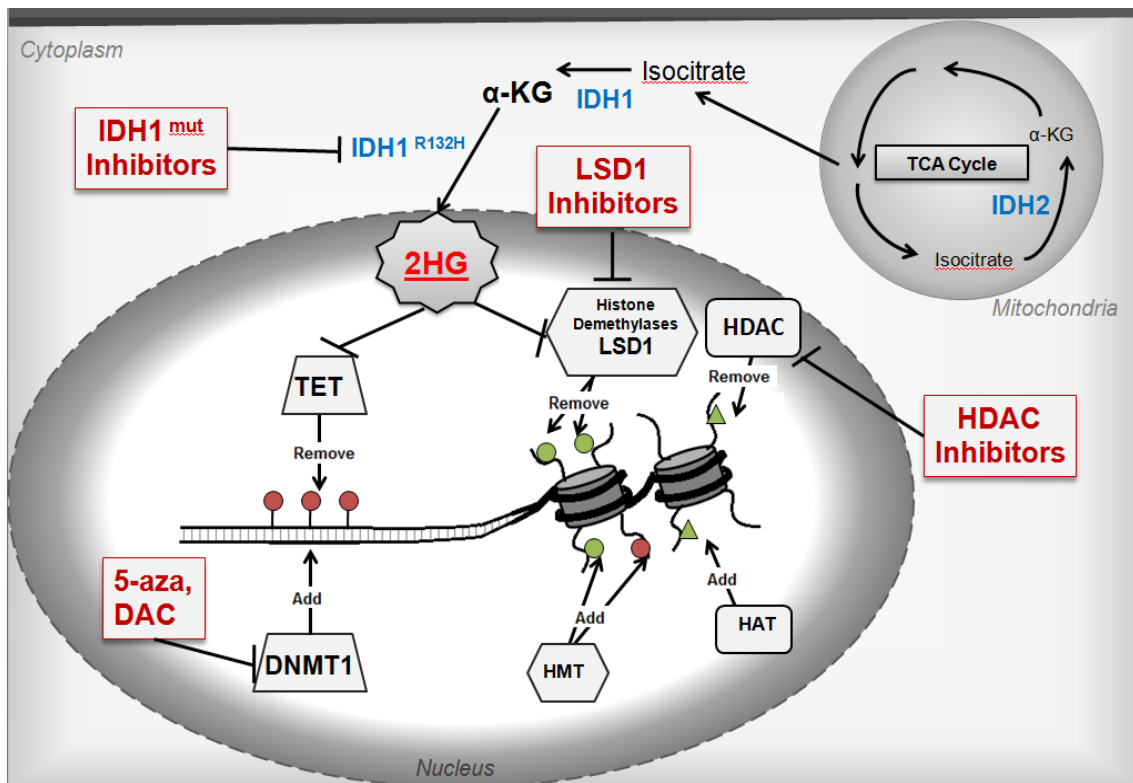


**Figure 4.3. Targeting epigenetic reprogramming caused by oncometabolite 2-HG.** Mutation in IDH1 leads to the accumulation of the oncometabolite 2-HG. Accumulation inhibits the TET family of enzymes believed to be involved in DNA demethylation and histone lysine demethylases. Targeting multiple components involved in epigenetic modification may lead to a synergistic effect *in vivo*.

## **Combination therapy with LSD1 inhibitors**

In addition to a reduction of histone acetylation, histone methylation is significantly increased in *IDH1* mutant gliomas. Lysine (K)-specific demethylase 1A (LSD1), a histone demethylase, is able to remove methylation marks H3K4me2 and H3K9me2. Studies have shown that increasing promoter H3K4me2 is associated with increasing levels of active gene transcription [93, 94]. Because LSD1 therefore has the capacity to repress gene expression at these areas, several novel LSD1 inhibitors have been developed which show single agent efficacy [95, 96]. Of most significance, the LSD1 inhibitors 2D and PG144 have both shown synergy with 5-azacytidine in an *in vivo* xenograft model of colorectal cancer [96]. This significant reduction of tumor burden was accompanied by increased H3K4 methylation and re-expression of silenced genes. Newly synthesized LSD1 inhibitors (2D, BP-107-15) are likely to exhibit synergize with DNA demethylating agents in *IDH1* mutant glioma by increasing the active histone markers H3K4me2 and H3K9me2 while simultaneously reducing repressive DNA methylation marks. At the time of writing, we are currently utilizing the flank JHH-273 model to determine the efficacy of combinatorial therapy of 5-aza and LSD1 inhibitors 2D and BP-107-15 on reduction of tumor burden. The single agent or combination that is most effective at reducing tumor burden will be validated in the JHH-273 orthotopic model and the BT142 *IDH1* mutant oligoastrocytoma orthotopic model. Additionally, the specificity of drug effect to *IDH1* mutant gliomas will be tested by repeating the study in the *IDH1* wild type intracranial model.

## **Determine the epigenetic and transcriptional alterations that are most useful for a successful therapeutic response**

In order to elucidate which epigenetic and transcriptional alterations are responsible for suppression of tumor growth, a rigorous evaluation of the tumors which exhibit a successful drug response will be necessary. We are currently examining the full methylation and transcriptional profiles of IDH1 mutant tumors treated with 5-aza at multiple treatment cycles. Briefly, RNA and gDNA was obtained from the JHH-273 flank tumors at each treatment cycle. Following bisulfate conversion of gDNA, methylation analysis will be performed using the Illumina Infinium HumanMethylation450 Beadchip which allows for analysis of >485,000 methylation sites.  $\beta$  values for treated tumors will be subtracted from the  $\beta$  values of the tumors treated with vehicle control. Any probe with  $\Delta\beta < -0.4$  will be considered to be hypomethylated following treatment.

To further address the functional consequences of epigenetic therapy, we will perform global gene expression analysis in flank tumors treated with 5-aza at each treatment cycle using a high-density oligonucleotide microarray (Agilent 4x44K Whole Human Genome Microarray). Transcriptional alterations will be subjected to Gene Set Enrichment Analysis (GSEA) with GSEA software v 2.0.14. We will assess the significance of the gene sets with an FDR Q-value cutoff of 25%. The most differentially expressed genes will be identified with the “leading edge subset” that consists of genes with the most contribution to the enrichment score of a particular gene set [97]. Knowledge of both transcriptional and epigenetic changes will allow us to integrate the two data sets to determine if reductions in gene methylation translate to increases in gene

transcription. To do this, we will first use an unsupervised variance analysis to assess the alterations in global gene expression after treatment. A one-way ANOVA analysis will then be performed on the data set to determine which transcripts significantly altered following treatment. Finally, we will analyze the two gene sets, consisting of hypomethylated and transcriptionally upregulated genes, using the Molecular Signature Database (MsigDB) to determine whether there is any overlap with curated gene sets. Additionally, we will employ gene ontology analyses for biological processes and molecular function using the DAVID bioinformatics resource [67]. This experimental strategy will allow us to correlate epigenetic and transcriptional changes to therapeutic response.

### **Investigate promising targets of successful therapeutic response.**

In order to determine which pathways and genes are responsible for a therapeutic response, we will perform functional genomics studies using *in vitro* systems. Using the methylome and transcriptome data, we will carefully demonstrate which genes are responsible for cell growth and differentiation using *IDH1* mutant cell lines and subsequent *in vivo* studies. The genetic targets which significantly increase expression following a loss of methylation may be involved in suppression of tumor growth and induction of cellular differentiation. Because the JHH-273 line is not amenable to cell culture, we will use the BT142 *IDH1* mutant oligoastrocytoma line for *in vitro* studies. BT142 cells will be transfected with siRNA constructs as well as scrambled siRNA controls to determine the consequences on cell proliferation, clonogenicity and capacity for differentiation, as described previously [39, 98]. As an additional control, we will use

the *IDH1* wild type Br23C neurosphere line transfected with identical siRNA constructs. This will inform us whether the effects are specific to *IDH1* mutant tumors or to gliomas as a whole. *In vitro* studies will then be validated in the *in vivo* model using intracranial implantations of the engineered cell lines. This will allow us to determine whether *in vitro* reductions in proliferation translate to *in vivo* reductions in tumor growth and extension of survival. Collectively the results of this study will allow us to reveal which molecular alterations are responsible for the suppression of tumor growth in *IDH1* mutant glioma.

### **Determine effect of demethylation therapy on populations of undifferentiated stem-like cells**

Stem cells rely on tightly controlled regulation of chromatin structure and DNA methylation to maintain homeostasis. Studies have shown that treatment of stem cells with epigenetic modulating agents induces changes in these cell populations [99]. For this reason, it is possible that treatment of the *IDH1* mutant gliomas with demethylating agents and epigenetic modulators may alter the population of undifferentiated stem-like cells, also called tumor initiating cells. In order to determine the effect of epigenetic modulation on the population of stem-like cells in the *IDH1* mutant tumors, we will use look at several putative cancer stem cell markers in those tumors which exhibit the strongest therapeutic response. JHH-273 flank tumors will be treated with 5-azacytidine for 3 treatment cycles. At the end of the third treatment cycle, flank tumors will be disassociated into a single cell suspension, fixed and stained using human specific fluorescent antibodies against CD133, Nestin and aldehyde dehydrogenase (ALDH). The

cells will then be subjected to flow cytometry analysis in order to quantify the change in stem-like cells. After gating for single, live cells populations, the undifferentiated stem-like cells will be measured as those which stain positive for CD133, Nestin and aldehyde dehydrogenase (CD133+/Nestin+/ALDH+). These results will be validated in the intracranial model in both the BT142 and the Br23C models using with immunohistochemical analysis using formalin fixed paraffin embedded tissue slides from treated and untreated intracranial tumor samples.

## REFERENCES

1. Parsons, D.W., et al., *An integrated genomic analysis of human glioblastoma multiforme*. Science, 2008. **321**(5897): p. 1807-12.
2. Yan, H., et al., *IDH1 and IDH2 mutations in gliomas*. N Engl J Med, 2009. **360**(8): p. 765-73.
3. Kim, J.W. and C.V. Dang, *Cancer's molecular sweet tooth and the Warburg effect*. Cancer Res, 2006. **66**(18): p. 8927-30.
4. Vander Heiden, M.G., L.C. Cantley, and C.B. Thompson, *Understanding the Warburg effect: the metabolic requirements of cell proliferation*. Science, 2009. **324**(5930): p. 1029-33.
5. Dang, C.V., A. Le, and P. Gao, *MYC-induced cancer cell energy metabolism and therapeutic opportunities*. Clin Cancer Res, 2009. **15**(21): p. 6479-83.
6. DeBerardinis, R.J., *Is cancer a disease of abnormal cellular metabolism? New angles on an old idea*. Genet Med, 2008. **10**(11): p. 767-77.
7. DeBerardinis, R.J., et al., *The biology of cancer: metabolic reprogramming fuels cell growth and proliferation*. Cell Metab, 2008. **7**(1): p. 11-20.
8. MacKenzie, E.D., et al., *Cell-permeating alpha-ketoglutarate derivatives alleviate pseudohypoxia in succinate dehydrogenase-deficient cells*. Mol Cell Biol, 2007. **27**(9): p. 3282-9.
9. King, A., M.A. Selak, and E. Gottlieb, *Succinate dehydrogenase and fumarate hydratase: linking mitochondrial dysfunction and cancer*. Oncogene, 2006. **25**(34): p. 4675-82.
10. Selak, M.A., et al., *Succinate links TCA cycle dysfunction to oncogenesis by inhibiting HIF-alpha prolyl hydroxylase*. Cancer Cell, 2005. **7**(1): p. 77-85.
11. Mardis, E.R., et al., *Recurring mutations found by sequencing an acute myeloid leukemia genome*. N Engl J Med, 2009. **361**(11): p. 1058-66.
12. Amary, M.F., et al., *IDH1 and IDH2 mutations are frequent events in central chondrosarcoma and central and periosteal chondromas but not in other mesenchymal tumours*. J Pathol, 2011. **224**(3): p. 334-43.



13. Sjoblom, T., et al., *The consensus coding sequences of human breast and colorectal cancers*. Science, 2006. **314**(5797): p. 268-74.
14. Kang, M.R., et al., *Mutational analysis of IDH1 codon 132 in glioblastomas and other common cancers*. Int J Cancer, 2009. **125**(2): p. 353-5.
15. Gaal, J., et al., *Isocitrate dehydrogenase mutations are rare in pheochromocytomas and paragangliomas*. J Clin Endocrinol Metab, 2010. **95**(3): p. 1274-8.
16. Borger, D.R., et al., *Frequent mutation of isocitrate dehydrogenase (IDH)1 and IDH2 in cholangiocarcinoma identified through broad-based tumor genotyping*. Oncologist, 2012. **17**(1): p. 72-9.
17. Sequist, L.V., et al., *Implementing multiplexed genotyping of non-small-cell lung cancers into routine clinical practice*. Ann Oncol, 2011. **22**(12): p. 2616-24.
18. Patnaik, M.M., et al., *WHO-defined 'myelodysplastic syndrome with isolated del(5q)' in 88 consecutive patients: survival data, leukemic transformation rates and prevalence of JAK2, MPL and IDH mutations*. Leukemia, 2010. **24**(7): p. 1283-9.
19. Thol, F., et al., *IDH1 mutations in patients with myelodysplastic syndromes are associated with an unfavorable prognosis*. Haematologica, 2010.
20. Thol, F., et al., *Prognostic impact of IDH2 mutations in cytogenetically normal acute myeloid leukemia*. Blood, 2010. **116**(4): p. 614-6.
21. Ward, P.S., et al., *The common feature of leukemia-associated IDH1 and IDH2 mutations is a neomorphic enzyme activity converting alpha-ketoglutarate to 2-hydroxyglutarate*. Cancer Cell, 2010. **17**(3): p. 225-34.
22. Dang, L., et al., *Cancer-associated IDH1 mutations produce 2-hydroxyglutarate*. Nature, 2009. **462**(7274): p. 739-44.
23. Zhao, S., et al., *Glioma-derived mutations in IDH1 dominantly inhibit IDH1 catalytic activity and induce HIF-1alpha*. Science, 2009. **324**(5924): p. 261-5.
24. Yang, B., et al., *Molecular mechanisms of "off-on switch" of activities of human IDH1 by tumor-associated mutation R132H*. Cell Res, 2010. **20**(11): p. 1188-200.

25. Kranendijk, M., et al., *Evidence for genetic heterogeneity in D-2-hydroxyglutaric aciduria*. Hum Mutat, 2010. **31**(3): p. 279-83.
26. Steenweg, M.E., et al., *An overview of L-2-hydroxyglutarate dehydrogenase gene (L2HGDH) variants: a genotype-phenotype study*. Hum Mutat, 2010. **31**(4): p. 380-90.
27. Struys, E.A., et al., *Mutations in phenotypically mild D-2-hydroxyglutaric aciduria*. Ann Neurol, 2005. **58**(4): p. 626-30.
28. Kranendijk, M., et al., *IDH2 mutations in patients with D-2-hydroxyglutaric aciduria*. Science, 2010. **330**(6002): p. 336.
29. Yazici, N., et al., *Glutaric aciduria type II [corrected] and brain tumors: a case report and review of the literature*. J Pediatr Hematol Oncol, 2009. **31**(11): p. 865-9.
30. Aghili, M., F. Zahedi, and E. Rafiee, *Hydroxyglutaric aciduria and malignant brain tumor: a case report and literature review*. J Neurooncol, 2009. **91**(2): p. 233-6.
31. Coskun, T., *L-2-hydroxyglutaric aciduria and brain tumors*. J Pediatr Hematol Oncol, 2010. **32**(4): p. 339-40; author reply 340.
32. Haliloglu, G., et al., *L-2-hydroxyglutaric aciduria and brain tumors in children with mutations in the L2HGDH gene: neuroimaging findings*. Neuropediatrics, 2008. **39**(2): p. 119-22.
33. Moroni, I., et al., *L-2-hydroxyglutaric aciduria and brain malignant tumors: a predisposing condition?* Neurology, 2004. **62**(10): p. 1882-4.
34. Struys, E.A., et al., *Mutations in the D-2-hydroxyglutarate dehydrogenase gene cause D-2-hydroxyglutaric aciduria*. Am J Hum Genet, 2005. **76**(2): p. 358-60.
35. Carter, H., et al., *Cancer-specific high-throughput annotation of somatic mutations: computational prediction of driver missense mutations*. Cancer Res, 2009. **69**(16): p. 6660-7.
36. Yan, H., et al., *Mutant metabolic enzymes are at the origin of gliomas*. Cancer Res, 2009. **69**(24): p. 9157-9.

37. Christensen, B.C., et al., *DNA methylation, isocitrate dehydrogenase mutation, and survival in glioma*. J Natl Cancer Inst, 2011. **103**(2): p. 143-53.
38. Reitman, Z.J., et al., *Profiling the effects of isocitrate dehydrogenase 1 and 2 mutations on the cellular metabolome*. Proc Natl Acad Sci U S A, 2011. **108**(8): p. 3270-5.
39. Seltzer, M.J., et al., *Inhibition of glutaminase preferentially slows growth of glioma cells with mutant IDH1*. Cancer Res, 2010. **70**(22): p. 8981-7.
40. Chowdhury, R., et al., *The oncometabolite 2-hydroxyglutarate inhibits histone lysine demethylases*. EMBO Rep, 2011. **12**(5): p. 463-9.
41. Gross, S., et al., *Cancer-associated metabolite 2-hydroxyglutarate accumulates in acute myelogenous leukemia with isocitrate dehydrogenase 1 and 2 mutations*. J Exp Med, 2010. **207**(2): p. 339-44.
42. Xu, W., et al., *Oncometabolite 2-hydroxyglutarate is a competitive inhibitor of alpha-ketoglutarate-dependent dioxygenases*. Cancer Cell, 2011. **19**(1): p. 17-30.
43. Loenarz, C. and C.J. Schofield, *Expanding chemical biology of 2-oxoglutarate oxygenases*. Nat Chem Biol, 2008. **4**(3): p. 152-6.
44. Figueroa, M.E., et al., *Leukemic IDH1 and IDH2 mutations result in a hypermethylation phenotype, disrupt TET2 function, and impair hematopoietic differentiation*. Cancer Cell, 2010. **18**(6): p. 553-67.
45. Turcan, S., et al., *IDH1 mutation is sufficient to establish the glioma hypermethylator phenotype*. Nature, 2012. **483**(7390): p. 479-83.
46. Noushmehr, H., et al., *Identification of a CpG island methylator phenotype that defines a distinct subgroup of glioma*. Cancer Cell, 2010. **17**(5): p. 510-22.
47. Slusher, B.S., et al., *Selective inhibition of NAALADase, which converts NAAG to glutamate, reduces ischemic brain injury*. Nat Med, 1999. **5**(12): p. 1396-402.
48. Wolf, A., S. Agnihotri, and A. Guha, *Targeting metabolic remodeling in glioblastoma multiforme*. Oncotarget, 2010. **1**(7): p. 552-62.
49. Koh, H.J., et al., *Cytosolic NADP<sup>+</sup>-dependent isocitrate dehydrogenase plays a key role in lipid metabolism*. J Biol Chem, 2004. **279**(38): p. 39968-74.

50. Aydin, K., et al., *Single-voxel MR spectroscopy and diffusion-weighted MRI in two patients with l-2-hydroxyglutaric aciduria*. *Pediatr Radiol*, 2003. **33**(12): p. 872-6.
51. Choi, C., et al., *2-hydroxyglutarate detection by magnetic resonance spectroscopy in IDH-mutated patients with gliomas*. *Nat Med*, 2012. **18**(4): p. 624-9.
52. Lu, C., et al., *IDH mutation impairs histone demethylation and results in a block to cell differentiation*. *Nature*, 2012. **483**(7390): p. 474-8.
53. Luchman, H.A., et al., *An in vivo patient-derived model of endogenous IDH1-mutant glioma*. *Neuro Oncol*, 2012. **14**(2): p. 184-91.
54. Klink, B., et al., *A novel, diffusely infiltrative xenograft model of human anaplastic oligodendroglioma with mutations in FUBP1, CIC, and IDH1*. *PLoS One*, 2013. **8**(3): p. e59773.
55. Siu, I.M., et al., *Establishment of a human glioblastoma stemlike brainstem rodent tumor model*. *J Neurosurg Pediatr*, 2010. **6**(1): p. 92-7.
56. Meeker, A.K., et al., *Telomere length assessment in human archival tissues: combined telomere fluorescence in situ hybridization and immunostaining*. *Am J Pathol*, 2002. **160**(4): p. 1259-68.
57. Montgomery, E., et al., *Telomere lengths of translocation-associated and nontranslocation-associated sarcomas differ dramatically*. *Am J Pathol*, 2004. **164**(5): p. 1523-9.
58. Chen, C., et al., *Single base discrimination of CENP-B repeats on mouse and human Chromosomes with PNA-FISH*. *Mamm Genome*, 1999. **10**(1): p. 13-8.
59. Vogelstein, B., et al., *Cancer genome landscapes*. *Science*, 2013. **339**(6127): p. 1546-58.
60. Heaphy, C.M., et al., *Altered telomeres in tumors with ATRX and DAXX mutations*. *Science*, 2011. **333**(6041): p. 425.
61. Borodovsky, A., et al., *5-azacytidine reduces methylation, promotes differentiation and induces tumor regression in a patient-derived IDH1 mutant glioma xenograft*. *Oncotarget*, 2013. **4**(10): p. 1737-47.

62. Silvestre, D.C., et al., *Alternative lengthening of telomeres in human glioma stem cells*. Stem Cells, 2011. **29**(3): p. 440-51.
63. Cihak, A., *Biological effects of 5-azacytidine in eukaryotes*. Oncology, 1974. **30**(5): p. 405-22.
64. Schneider-Stock, R., et al., *5-Aza-cytidine is a potent inhibitor of DNA methyltransferase 3a and induces apoptosis in HCT-116 colon cancer cells via Gadd45- and p53-dependent mechanisms*. J Pharmacol Exp Ther, 2005. **312**(2): p. 525-36.
65. Jin, G., et al., *Disruption of wild-type IDH1 suppresses D-2-hydroxyglutarate production in IDH1-mutated gliomas*. Cancer Res, 2012. **73**(2): p. 496-501.
66. Trembath, D.G., et al., *A novel small molecule that selectively inhibits glioblastoma cells expressing EGFRvIII*. Mol Cancer, 2007. **6**: p. 30.
67. Turcan, S., et al., *Efficient Induction of Differentiation and Growth Inhibition in IDH1 Mutant Glioma Cells by the DNMT Inhibitor Decitabine*. Oncotarget, 2013.
68. Duncan, C.G., et al., *A heterozygous IDH1R132H/WT mutation induces genome-wide alterations in DNA methylation*. Genome Res, 2012. **22**(12): p. 2339-55.
69. Lu, C., et al., *IDH mutation impairs histone demethylation and results in a block to cell differentiation*. Nature. **483**(7390): p. 474-8.
70. Chou, A.P., et al., *Identification of retinol binding protein 1 promoter hypermethylation in isocitrate dehydrogenase 1 and 2 mutant gliomas*. J Natl Cancer Inst, 2012. **104**(19): p. 1458-69.
71. Kaiser, M.F., et al., *Global methylation analysis identifies prognostically important epigenetically inactivated tumor suppressor genes in multiple myeloma*. Blood, 2013. **122**(2): p. 219-26.
72. Choi, Y.J., et al., *Aberrant expression of SOX9 is associated with gastrosine 1 inactivation in gastric cancers*. Gastric Cancer, 2013(DOI 10.1007/s10120-013-0277-3).
73. Bao, Z., et al., *BMP4, a strong better prognosis predictor, has a subtype preference and cell development association in gliomas*. J Transl Med, 2013. **11**: p. 100.

74. Lombardo, Y., et al., *Bone morphogenetic protein 4 induces differentiation of colorectal cancer stem cells and increases their response to chemotherapy in mice*. *Gastroenterology*, 2011. **140**(1): p. 297-309.
75. Stone, A.R., et al., *Aberrant methylation and down-regulation of TMS1/ASC in human glioblastoma*. *Am J Pathol*, 2004. **165**(4): p. 1151-61.
76. Kordi Tamandani, D.M., et al., *CpG island methylation of TMS1/ASC and CASP8 genes in cervical cancer*. *Eur J Med Res*, 2009. **14**: p. 71-5.
77. Kunwar, S., et al., *Genetic subgroups of anaplastic astrocytomas correlate with patient age and survival*. *Cancer Res*, 2001. **61**(20): p. 7683-8.
78. Easwaran, H., et al., *A DNA hypermethylation module for the stem/progenitor cell signature of cancer*. *Genome Res*, 2012. **22**(5): p. 837-49.
79. Chabot, G.G., G.E. Rivard, and R.L. Momparler, *Plasma and cerebrospinal fluid pharmacokinetics of 5-Aza-2'-deoxycytidine in rabbits and dogs*. *Cancer Res*, 1983. **43**(2): p. 592-7.
80. Tsai, H.C., et al., *Transient low doses of DNA-demethylating agents exert durable antitumor effects on hematological and epithelial tumor cells*. *Cancer Cell*, 2012. **21**(3): p. 430-46.
81. Hegi, M.E., et al., *Clinical trial substantiates the predictive value of O-6-methylguanine-DNA methyltransferase promoter methylation in glioblastoma patients treated with temozolomide*. *Clin Cancer Res*, 2004. **10**(6): p. 1871-4.
82. Hashimshony, T., et al., *The role of DNA methylation in setting up chromatin structure during development*. *Nat Genet*, 2003. **34**(2): p. 187-92.
83. Kim, H.J., et al., *DNMT (DNA methyltransferase) inhibitors radiosensitize human cancer cells by suppressing DNA repair activity*. *Radiat Oncol*, 2012. **7**: p. 39.
84. Rohle, D., et al., *An inhibitor of mutant IDH1 delays growth and promotes differentiation of glioma cells*. *Science*, 2012. **340**(6132): p. 626-30.
85. Soriano, A.O., et al., *Safety and clinical activity of the combination of 5-azacytidine, valproic acid, and all-trans retinoic acid in acute myeloid leukemia and myelodysplastic syndrome*. *Blood*, 2007. **110**(7): p. 2302-8.

86. Prebet, T., et al., *Combination of vorinostat and low dose cytarabine for patients with azacitidine-refractory/relapsed high risk myelodysplastic syndromes*. Leuk Res, 2013.
87. Brodska, B., et al., *Combined Treatment with Low Concentrations of Decitabine and SAHA Causes Cell Death in Leukemic Cell Lines but Not in Normal Peripheral Blood Lymphocytes*. Biomed Res Int, 2013. **2013**: p. 659254.
88. Pfeiffer, M.M., et al., *Influence of Histone Deacetylase Inhibitors and DNA-Methyltransferase Inhibitors on the NK Cell-Mediated Lysis of Pediatric B-Lineage Leukemia*. Front Oncol, 2013. **3**: p. 99.
89. Chen, M.Y., et al., *Decitabine and suberoylanilide hydroxamic acid (SAHA) inhibit growth of ovarian cancer cell lines and xenografts while inducing expression of imprinted tumor suppressor genes, apoptosis, G2/M arrest, and autophagy*. Cancer, 2011. **117**(19): p. 4424-38.
90. Zhu, X., Y. Ma, and D. Liu, *Novel agents and regimens for acute myeloid leukemia: 2009 ASH annual meeting highlights*. J Hematol Oncol, 2010. **3**: p. 17.
91. Belinsky, S.A., et al., *Combination therapy with vidaza and entinostat suppresses tumor growth and reprograms the epigenome in an orthotopic lung cancer model*. Cancer Res, 2011. **71**(2): p. 454-62.
92. Juergens, R.A., et al., *Combination epigenetic therapy has efficacy in patients with refractory advanced non-small cell lung cancer*. Cancer Discov, 2011. **1**(7): p. 598-607.
93. Liang, G., et al., *Distinct localization of histone H3 acetylation and H3-K4 methylation to the transcription start sites in the human genome*. Proc Natl Acad Sci U S A, 2004. **101**(19): p. 7357-62.
94. McGarvey, K.M., et al., *Defining a chromatin pattern that characterizes DNA-hypermethylated genes in colon cancer cells*. Cancer Res, 2008. **68**(14): p. 5753-9.
95. Wang, J., et al., *Novel histone demethylase LSD1 inhibitors selectively target cancer cells with pluripotent stem cell properties*. Cancer Res, 2011. **71**(23): p. 7238-49.

96. Huang, Y., et al., *Novel oligoamine analogues inhibit lysine-specific demethylase 1 and induce reexpression of epigenetically silenced genes*. Clin Cancer Res, 2009. **15**(23): p. 7217-28.
97. Subramanian, A., et al., *Gene set enrichment analysis: a knowledge-based approach for interpreting genome-wide expression profiles*. Proc Natl Acad Sci U S A, 2005. **102**(43): p. 15545-50.
98. Baia, G.S., et al., *Yes-associated protein 1 is activated and functions as an oncogene in meningiomas*. Mol Cancer Res, 2012. **10**(7): p. 904-13.
99. Schmittwolf, C., et al., *In vivo haematopoietic activity is induced in neurosphere cells by chromatin-modifying agents*. EMBO J, 2005. **24**(3): p. 554-66.

## CURRICULUM VITAE

### **Alexandra Borodovsky**

Department of Neurosurgery, Sidney Kimmel Comprehensive Cancer Center  
The Johns Hopkins University School of Medicine  
1650 Orleans Street, Cancer Research Building 1, Room 276, Baltimore, Maryland,  
21287  
Home: 503-490-7415 Work: 410-502-2908  
Email: [aborodo1@jhmi.edu](mailto:aborodo1@jhmi.edu)

---

### **EDUCATION**

**Ph.D.**                      **Cellular and Molecular Medicine**                      **2013**  
The Johns Hopkins University School of Medicine, Baltimore, Maryland  
**Dissertation:** Modeling and Therapeutic Targeting of Endogenous *IDH1* mutant glioma  
Advisor: Gregory J. Riggins, M.D, Ph.D.

**B.S.**                      **Molecular and Cellular Biology**                      **2008**  
University of Puget Sound, Tacoma, WA  
Graduated with University Honors, GPA 3.56/4.0  
**Thesis:** The Effects of Progesterone and Wnt3a on the Wnt Signaling Pathway  
Advisor: Alyce DeMarais, Ph.D.

### **RESEARCH EXPERIENCE**

**Doctoral Research**                      September 2009-present  
Johns Hopkins University, School of Medicine, Baltimore, MD

- Development of a novel patient-derived *IDH1* mutant glioma xenograft model
- Preclinical studies of a targeted therapy for the treatment of glioma involving



- mutations in isocitrate dehydrogenase 1 (IDH1)
- Utilized cell-based and murine assays to study efficacy in glioma cell lines and primary patient samples
- Studied perturbation of tumor growth in mouse models of *IDH1* mutant glioma.
- Research was focused on inducing differentiation and reducing proliferation using FDA approved demethylating compounds

**Research Associate** May 2008-July 2009  
Earle A. Chiles Research Institute, Providence Medical Center, Portland OR

- Investigated the pro-apoptotic mechanisms of  $\alpha$ -tocopheryloxyacetic acid ( $\alpha$ -TEA) on human and murine cancer cells.
- Utilized flow cytometry and Western blotting to show that  $\alpha$ -TEA promotes mitochondrial membrane depolarization and subsequent generation of radical oxygen species in a variety of human cancer cell lines.
- Investigated the synergistic effects of lapatinib and  $\alpha$ -TEA in HER2 positive breast cancer.
- Studied the prophylactic effects of  $\alpha$ -TEA in a mouse model of breast cancer.

**Research Assistant** May 2007-August 2007  
Department of Ob/Gyn & Reproductive Sciences, University of California, San Francisco, San Francisco CA

- Verified the results of a microarray study investigating the effects of Wnt treatment on target gene transcription.
- Confirmed the effects of Wnt3a on the Wnt signaling pathway using Q-PCR, ELISA and Western blot analysis on decidualized and non-decidualized human endometrial stromal cells.

**Research Assistant** January 2006-May 2008  
Department of Biology, University of Puget Sound, Tacoma, WA

- Studied the effects of progesterone on components of the Wnt signaling pathway in zebrafish and mosquitofish oocytes.
- Identified that progesterone promotes translocation of membrane bound  $\beta$ -catenin to the nucleus in zebrafish and increases *GSK3 $\beta$*  transcription in mosquitofish

## ADDITIONAL EXPERIENCE

**Departmental Representative for the Graduate Student Association** August 2010-  
August 2013  
Johns Hopkins University, School of Medicine, Baltimore MD

- Worked collaboratively with members of the Graduate Student Association to organize graduate events, assist in policy reform.
- Represented the interests of the departmental student body at general meetings.

**President, Phi Sigma Biological Honors Society** August 2007-May 2008  
University of Puget Sound, Tacoma, WA

- Organized and led the 2008 Phi Sigma Research Symposium.
- Coordinated environmental and educational outreach programs.
- Directed bimonthly meetings.

**Science Writing Advisor**

August 2007- May 2008

University of Puget Sound, Tacoma, WA

- Guided graduate and undergraduate students in all components of the writing process with an emphasis on scientific writing.
- Educated students on writing techniques and conventions present in various writing styles.

**Biology Teaching Assistant**

August 2006-December 2006

University of Puget Sound, Tacoma, WA

- Assisted students in the design and execution of experiments and graded quizzes and assignments.
- Mediated the team-work process and resolved student conflicts concerning design and distribution of work.

**AWARDS AND HONORS**

- Departmental Honors in Molecular and Cellular Biology, 2008
- Dean's List, University of Puget Sound, Fall 2007-Spring 2008
- Summer Research Grant, University of Puget Sound, Spring 2007
- Enrichment Committee Grant for Undergraduate Research, 2006-2008

**INTELLECTUAL PROPERTY**

2013 License of intellectual property of *IDH1* mutant glioma xenograft (JHH-273) for commercial distribution

**PUBLICATIONS**

**Borodovsky, A,** Meeker, AK, Kirkness, EF, Zhao, Q, Eberhart, CG, Gallia GL, Riggins, GJ. A novel model of a patient-derived IDH1 mutant gliomas with alternative lengthening of telomeres. (*In review*).

**Borodovsky A,** Salmasi V, Turcan S, Fabius AW, Baia GS, Eberhart CG, Weingart JD, Gallia GL, Baylin SB, Chan TA, Riggins GJ. 5-azacytidine reduces methylation, promotes differentiation and induces tumor regression in a patient-derived IDH1 mutant glioma xenograft. *Oncotarget*. 2013;4(10):1737-47

**Borodovsky A**, Seltzer MJ, Riggins GJ. Altered cancer cell metabolism in gliomas with mutant IDH1 or IDH2. *Curr Opin Oncol*. 2012;24(1):83-9.

Turcan S, Fabius AW, **Borodovsky A**, Pedraza A, Brennan C, Huse J, et al. Efficient induction of differentiation and growth inhibition in IDH1 mutant glioma cells by the DNMT Inhibitor Decitabine. *Oncotarget*. 2013;4(10):1729-36. PMID: 3858559.

Kim J, Aftab BT, Tang JY, Kim D, Lee AH, Rezaee M, Rezaee M, Kim J, Chen B, King EM, **Borodovsky A**, Riggins GJ, Epstein EH Jr, Beachy PA, Rudin CM. Itraconazole and arsenic trioxide inhibit Hedgehog pathway activation and tumor growth associated with acquired resistance to smoothened antagonists. *Cancer Cell*. 2013;23(1):23-34. PMID: 3548977.

Hahn T, Polanczyk MJ, **Borodovsky A**, Ramanathapuram LV, Akporiaye ET, Ralph SJ. Use of anti-cancer drugs, mitocans, to enhance the immune responses against tumors. *Curr Pharm Biotechnol*. 2013;14(3):357-76. PMID: 3827888.

## REFERENCES

Gregory J. Riggins, MD, PhD  
Professor of Neurosurgery and Oncology  
Irving J. Sherman Research Professor,  
Johns Hopkins School of Medicine  
Address: CRB2 276  
1550 Orleans St, Baltimore MD 21287  
Email: griggin1@jhmi.edu  
Phone: 410-502-2904